

New Pyrazole-Based Ligands with Two Tripodal Binding Pockets: Potential Scaffolds for Metallobiosite Modeling

Holger Müller,[†] Bernhard Bauer-Siebenlist,[†] Edit Csapo,[‡] Sebastian Dechert,[†] Etelka Farkas,[‡] and Franc Meyer^{*†}

Institut für Anorganische Chemie, Georg-August-Universität, Tammannstrasse 4, D-37077 Göttingen, Germany, and Department of Inorganic and Analytical Chemistry, Faculty of Science, University of Debrecen, H-4010 Debrecen, Hungary

Received February 7, 2008

The synthesis of a new set of bioinspired dinucleating ligand scaffolds HL¹–HL³ based on a bridging pyrazolate with appended chelate arms is reported. The ligands provide two binding compartments akin to the tris(imidazolyl)methane motif, predisposed to act as facially tridentate coordination caps. Potentiometric titrations of HL¹ in the presence of Ni²⁺ and Zn²⁺ reveal formation of species with a metal:ligand ratio 1:1 in aqueous solution, and UV–vis data for the Ni^{II} system suggest that the complex [L¹₂Ni₂]²⁺ with {NiN₆} chromophore is formed under appropriate pH conditions. In contrast, trinickel(II) complexes [L²₂Ni₃(NO₃)₄(MeOH)₂] (**4**) and [L²₂Ni₃Cl₂(MeOH)₄]Cl₂ (**5**) could be obtained from MeOH solutions and characterized crystallographically. The anticipated tripodal {N₃} binding mode of the ligand is indeed realized for the central Ni^{II} ion, but the counteranions or MeOH solvent molecules lead to dissociation of one of the N donor legs for the outer Ni^{II} ions with formation of intramolecular H-bonds between a Ni-bound MeOH and the pyrazolate-N. X-ray crystal structures were also obtained for three Cu^I complexes [L³₂Cu₄X₂](PF₆)₂ with X = PMe₃ (**6**), CN*n*Bu (**7**), CNC₆H₃Me₂-2,6 (**8**), where all Cu^I ions are three-coordinate in a distorted trigonal-planar arrangement. The two inner metals are bound to two imidazole-N from one ligand sidearm and a pyrazolate-N from the other ligand while the outer Cu^I ions are hosted by the pyrazolate-N and one imidazole-N from the nearby sidearm with the third coordination site filled by the coligand X. Spectroscopic and ESI-MS data suggest that the trinickel complexes stay intact even in coordinating solvents while the Cu^I complexes in solution are partly dissociated into their bimetallic constituents. The solid state structures observed for the oligonuclear complexes **4**–**8** are reminiscent of the coordination motifs previously found for related mononuclear complexes based on tripodal tris(imidazolyl)methane, which corroborates the description of HL¹–HL³ as novel binucleating versions of such tris(imidazolyl)methane ligands.

Introduction

Through coordination of its two N atoms the pyrazolate heterocycle may span two metal ions, and hence, it is well established as an anionic bridging unit in bi- and polynuclear complexes, usually supporting metal–metal separations in the range 3.0–4.5 Å.¹ Further elaboration of pyrazolate coordination chemistry and increased preorganization can be achieved by attaching chelating side arms to the 3- and

5-positions of the heterocycle.² This strategy allows one to control crucial parameters of the resulting bimetallic scaffold such as, inter alia, the coordination number of the individual metal ions or the metal–metal distance.³ Selected examples of compartmental pyrazolate-derived ligands are shown in Scheme 1.

* To whom correspondence should be addressed. E-mail: franc.meyer@chemie.uni-goettingen.de. Telephone: ++49-551-393012. Fax: ++49-551-393063.

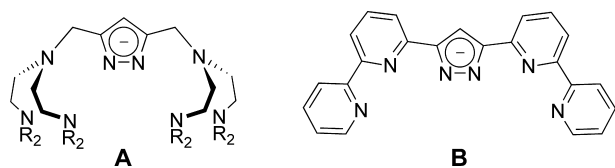
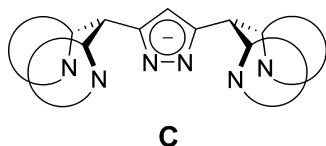
[†] Georg-August-Universität Göttingen.

[‡] University of Debrecen.

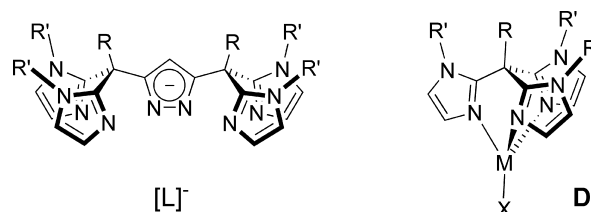
(1) (a) Trofimenko, S. *Prog. Inorg. Chem.* **1986**, *34*, 115–210. (b) La Monica, G.; Ardizzoia, G. A. *Prog. Inorg. Chem.* **1997**, *46*, 151–238.

(2) (a) Mukherjee, R. N. *Coord. Chem. Rev.* **2000**, *203*, 151–218. (b) Gavrilova, A. L.; Bosnich, B. *Chem. Rev.* **2004**, *104*, 349–383.

(3) (a) Meyer, F.; Heinze, K.; Nuber, B.; Zsolnai, L. *J. Chem. Soc., Dalton Trans.* **1998**, 207–213. (b) Konrad, M.; Meyer, F.; Heinze, K.; Zsolnai, L. *J. Chem. Soc., Dalton Trans.* **1998**, 199–205. (c) Ackermann, J.; Meyer, F.; Pritzkow, H. *Inorg. Chim. Acta* **2004**, *357*, 3703–3711. (d) Prokofieva, A.; Prikhodko, A. I.; Enyedy, E. A.; Farkas, E.; Maringele, W.; Demeshko, S.; Dechert, S.; Meyer, F. *Inorg. Chem.* **2007**, *46*, 4298–4307.

Scheme 1. Pyrazolate-Derived Ligands Used in Previous Work^{4,5}**Scheme 2.** Schematic Representation of the Targeted Ligand Type C

Systems **A** consist of two tripodal tetradentate binding pockets of the tris(aminoalkyl)amine type that favor trigonal bipyramidal metal ion coordination.⁴ The rigid type **B** system provides two sites with planar {N₃} ligation, suitable for square-planar metal ion environments or a meridional {N₃} arrangement in [2 × 2] grid-complexes with six-coordinate vertices.⁵ Ligands of type **A** and related ones have been successfully employed for functional modeling of binuclear metalloenzyme active sites, mimicking the active sites of dizinc hydrolases,⁶ the dinickel enzyme urease,⁷ or type 3 dicopper enzymes.⁸ However, metal ions in many of these biological systems (such as the type 3 dicopper sites) are bound to only three N atoms of the surrounding protein matrix, usually to three facially disposed histidine-N.⁹ This situation is clearly different from the tripodal tetradentate arrangement of four N-donors in **A**. Improved structural emulation of the biological counterparts may thus be expected from novel pyrazolate-based scaffolds of generic type **C** (Scheme 2) that provide two facially tridentate metal ion binding sites reminiscent of the biological {His}₃ motif. Here we report a synthetic approach to some first ligands with a type **C** framework and their basic coordination chemistry.

Scheme 3. Ligands of Type [L]⁻ Are Descended from Tris(imidazolyl)methanes **D**

Results and Discussion

Synthesis and Characterization of Ligands. Given the spatial arrangement of the donor atoms in the sought-after type **C** compounds we devised a synthetic approach to potential ligands [L]⁻ (Scheme 3), in which two pendant imidazole groups are attached to quaternary bridgehead carbon atoms hooked to the 3- and 5-positions of the central pyrazole core. Each of the two {N₃} compartments of [L]⁻ would resemble the well-known facially tridentate tris(imidazolyl)methane motif that can support tetrahedral type **D** complexes (Scheme 3),^{10–13} similar to the related tris(pyrazolyl)borates.¹⁴

Three new pyrazole ligands HL¹, HL², and HL³ have been obtained that differ by the imidazole backbone substituents. Their synthesis was developed in close analogy to procedures reported previously for related ligands but lacking the central pyrazole (Scheme 4).¹⁵ The starting material in the present case is tetrahydropyranyl (thp) protected dimethylpyrazole-3,5-dicarboxylate **1**, which can be obtained in three steps from 3,5-dimethylpyrazole.¹⁶ Diester **1** was converted into dialcohols **2a–c** by nucleophilic attack of the carbanion generated from different *N*-methyl imidazoles. The three derivatives *N*-methylimidazole, 1,4,5-trimethylimidazole, and 4,5-diphenyl-*N*-methylimidazole have been chosen to finally provide HL¹, HL², and HL³, respectively. Compound **2a** could be crystallized from tetrahydrofuran (THF), and its molecular structure was determined crystallographically to confirm the anticipated constitution (Supporting Information, Figure S1). Alcohol functions at the bridgehead C atoms of

(4) (a) Meyer, F.; Beyreuther, S.; Heinze, K.; Zsolnai, L. *Chem. Ber./Recl.* **1997**, *130*, 605–613. (b) Siegfried, L.; Kaden, T. A.; Meyer, F.; Kircher, P.; Pritzkow, H. *J. Chem. Soc., Dalton Trans.* **2001**, 2310–2315. (c) Alvarinho Gil, M.; Maringele, W.; Dechert, S.; Meyer, F. *Z. Anorg. Allg. Chem.* **2007**, *633*, 2178–2186.

(5) van der Vlugt, J. I.; Demeshko, S.; Dechert, S.; Meyer, F. *Inorg. Chem.* **2008**, *47*, 1576–1585.

(6) (a) Meyer, F.; Rutsch, P. *Chem. Commun.* **1998**, 1037–1038. (b) Bauer-Siebenlist, B.; Meyer, F.; Farkas, E.; Vidovic, D.; Seijo, J. A. C.; Herbst-Irmer, R.; Pritzkow, H. *Inorg. Chem.* **2004**, *43*, 4189–4202. (c) Bauer-Siebenlist, B.; Meyer, F.; Farkas, E.; Vidovic, D.; Dechert, S. *Chem.—Eur. J.* **2005**, *11*, 4349–4360. (d) Bauer-Siebenlist, B.; Dechert, S.; Meyer, F. *Chem.—Eur. J.* **2005**, *11*, 5343–5352. (e) Meyer, F. *Eur. J. Inorg. Chem.* **2006**, 3789–3800.

(7) (a) Meyer, F.; Pritzkow, H. *Chem. Commun.* **1998**, 1555–1556. (b) Meyer, F.; Kaifer, E.; Kircher, P.; Heinze, K.; Pritzkow, H. *Chem.—Eur. J.* **1999**, *5*, 1617–1630. (c) Konrad, M.; Meyer, F.; Jacobi, A.; Kircher, P.; Rutsch, P.; Zsolnai, L. *Inorg. Chem.* **1999**, *38*, 4559–4566. (d) Buchler, S.; Meyer, F.; Pritzkow, H. *Inorg. Chim. Acta* **2002**, *337*, 371–386. (e) Kryatov, S. V.; Rybak-Akimova, E. V.; Meyer, F.; Pritzkow, H. *Eur. J. Inorg. Chem.* **2003**, 1581–1590.

(8) (a) Meyer, F.; Pritzkow, H. *Angew. Chem.* **2000**, *112*, 2199–2202; *Angew. Chem., Int. Ed.* **2000**, *39*, 2112–2115. (b) Ackermann, J.; Meyer, F.; Kaifer, E.; Pritzkow, H. *Chem.—Eur. J.* **2002**, *8*, 247–258. (c) Ackermann, J.; Buchler, S.; Meyer, F. *C.R. Chim.* **2007**, *10*, 421–432.

(9) (a) Klabunde, T.; Eicken, C.; Sacchettini, J. C.; Krebs, B. *Nat. Struct. Biol.* **1998**, *5*, 1084–1090. (b) Matoba, Y.; Kumagai, T.; Yamamoto, A.; Yoshitsu, H.; Sugiyama, M. *J. Biol. Chem.* **2006**, *13*, 8981–8990.

(10) Sorrell, T. N.; Borovik, A. S. *J. Am. Chem. Soc.* **1987**, *109*, 4255–4260.

(11) (a) Elgafi, S.; Field, L. D.; Messerle, B. A.; Buys, I. E.; Hambley, T. W. *J. Organomet. Chem.* **1997**, *309*, 119–128. (b) Wu, L. P.; Yamagiwa, Y.; Ino, I.; Sugimoto, K.; Kuroda-Sowa, T.; Kamikawa, T.; Munakata, M. *Polyhedron* **1999**, *18*, 2047–2053.

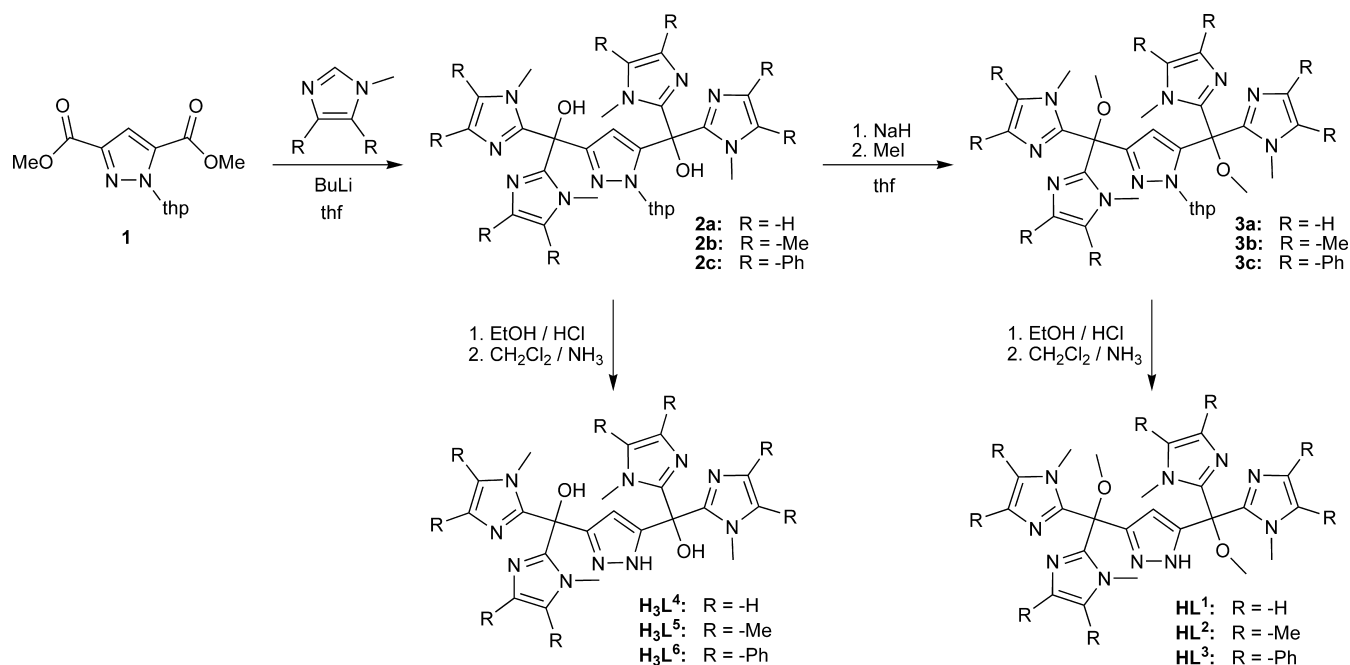
(12) Higgs, T. C.; Helliwell, M.; McInnes, E. J. L.; Mabbs, F. E.; Harding, C. J.; Garner, C. D. *J. Chem. Soc., Dalton Trans.* **1997**, 927–933.

(13) Zhou, L.; Powell, D.; Nicholas, K. M. *Inorg. Chem.* **2007**, *46*, 2316–2321.

(14) (a) Trofimenko, S. *Chem. Rev.* **1993**, *93*, 943–980. (b) Trofimenko, S. *Polyhedron* **2004**, *23*, 197–203.

(15) (a) Tang, C. C.; Davalian, D.; Huang, P.; Breslow, R. *J. Am. Chem. Soc.* **1998**, *120*, 3918–3922. (b) Takano, S.; Yano, Y.; Tagaki, W. *Chem. Lett.* **1981**, 1177–1180. (c) Breslow, R.; Hunt, J. T.; Smiley, R.; Tamowski, T. *J. Am. Chem. Soc.* **1983**, *105*, 5337–5342. (d) Tamagaki, S.; Kanamaru, Y.; Ueno, M.; Tagaki, W. *Bull. Chem. Soc. Jpn.* **1991**, *64*, 165–174. (e) Kesicki, E. A.; Derosch, M. A.; Freeman, L. H.; Walton, C. L.; Harvey, D. F.; Trogler, W. C. *Inorg. Chem.* **1993**, *32*, 5851–5867. (f) Kondo, S.-I.; Shinbo, K.; Yamaguchi, T.; Yoshida, K.; Yano, Y. *J. Chem. Soc., Perkin Trans.* **2001**, *1*, 128–131. (g) Worm, K.; Chu, F. Y.; Matsumoto, K.; Best, M. D.; Lynch, V.; Anslyn, E. V. *Chem.—Eur. J.* **2003**, *9*, 741–747.

(16) Röder, J. C.; Meyer, F.; Konrad, M.; Sandhöfner, S.; Kaifer, E.; Pritzkow, H. *Eur. J. Org. Chem.* **2001**, *2001*, 4479–4487.

Scheme 4. Synthesis of Ligands HL¹, HL², HL³ and H₃L⁴, H₃L⁵, H₃L⁶

2a–c were then methylated, followed by removal of the thp protection group under acidic conditions to afford the hydrochloride salts of HL,¹ HL,² and HL,³ which were finally neutralized. Isolation of the compound derived from *N*-methylimidazole (HL¹) required Soxhlet-extraction with diethyl ether, with the drawback that small residual amounts of the solvent cannot be removed from the product even after prolonged heating to 65 °C under reduced pressure. It is assumed that the presence of both H-bond donor and acceptor sites causes the new compounds to tightly retain polar (in particular protic) solvent molecules in the otherwise pure products.

An additional set of potentially triprotic ligands H₃L⁴, H₃L⁵, and H₃L⁶ could be obtained by directly deprotecting **2a–c** without methylation of the backbone-OH. Possible deprotonation of the alcohol functions and their involvement in metal ion coordination may severely complicate any coordination chemistry of these latter systems, however, as was already seen in related tris(imidazolyl)methane systems.¹²

Ni²⁺, Cu⁺, and Zn²⁺ were chosen for the present study to assess whether the new ligands might act as bridging ligands and provide two facially disposed {N₃} donor sets in the anticipated way, since all these three metal ions are known to potentially form tetrahedral or octahedral complexes supported by tripodal coordination caps. Using parent HL¹ as an example, potentiometric titrations were carried out to determine the p*K*_a values of this new ligand and to probe its coordination chemistry toward Ni²⁺ and Zn²⁺ in solution.¹⁷

Ligand Protonation Constants. Titrations were performed starting at acidic pH using a potassium hydroxide titrant. From the titration curves, the deprotonation steps can

Table 1. Overall Protonation Constants (log β) and Sequential Dissociation Constants (p*K*_a) of the Ligand HL¹ at 25 °C with *I* = 0.2 M (KCl)^a

	[H ₅ L ¹] ⁴⁺	[H ₄ L ¹] ³⁺	[H ₃ L ¹] ²⁺	[H ₂ L ¹] ⁺
log β	14.67(7)	13.26(5)	10.72(3)	5.92(2)
p <i>K</i> _a	1.41(1)	2.54(1)	4.80(1)	5.92(1)

^a Standard deviations are given in parenthesis.

be derived (Supporting Information, Figure S3 and Table 1). The processes occurring in the measurable pH range between pH 2 and 11 correspond to the dissociation of one proton per protonated imidazole moiety. The differences between the sequential dissociation constants are higher than expected for statistical reasons, indicating some interaction between the individual protonation sites. Remarkably, the differences between the first and second as well as third and fourth p*K*_a are very similar (1.12 units), but the difference between the second and third protonation step is considerably higher (2.36 units). It can be assumed that one imidazole ring in each compartment of the ligand is protonated first while protonation of the proximate second imidazole of each subunit only takes place at much lower pH. Protonation of the pyrazole to the corresponding hydrochloride to give [H₆L¹]⁵⁺ could not be observed because this process occurs even below pH 2.

Species Distribution of Ni²⁺ and Zn²⁺ Complexes.

Titration of HL¹ in the presence of various equivalents of Ni²⁺ or Zn²⁺ were analyzed in batch calculations in which all titrations are fitted at the same time with one model (Supporting Information, Figures S4 and S5, and Tables 2, 3). Interestingly, only species with a 1:1 ligand to metal ratio could be detected in aqueous solution. This is evident from the coincidence of the titration curves obtained for Ni²⁺ and Zn²⁺ at 1:1 and 1:2 ligand to metal ratios below the pH where hydrolysis of the excess of metal ion starts.

At low pH free Zn²⁺ and small amounts of species [H₃L¹Zn]⁴⁺ and [H₂L¹Zn]³⁺ are present, which are probably

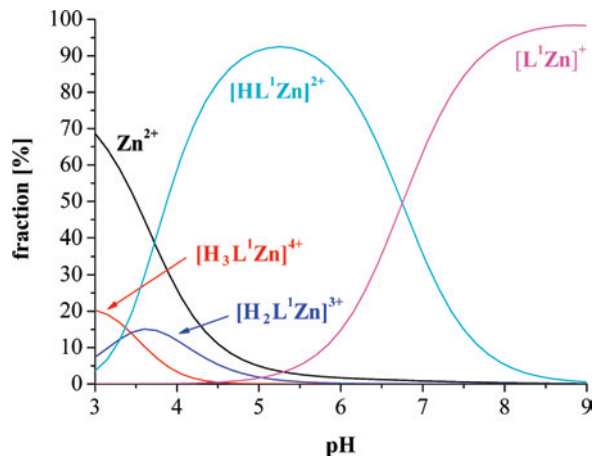
(17) Cu²⁺ was deemed to be unsuited for the present purpose because it does not form tetrahedral complexes but strongly favors tetragonal coordination environments. The species distribution of HL¹ with Cu⁺ in aqueous solution could not be determined because the resulting complexes exhibit low stability in water.

Table 2. Overall Stability Constants ($\log \beta$) and Dissociation Constants (pK) for the Complexes formed with Ni^{2+} at 25 °C with $I = 0.2$ M (KCl)^a

	$[H_2L^1Ni]^{3+}$	$[HL^1Ni]^{2+}$	$[L^1Ni]^+$	$[L^1_{-H}Ni]$
$\log \beta$	12.14(3)	9.82(2)	0.84(6)	-9.98(8)
pK	2.32	8.98	10.82	

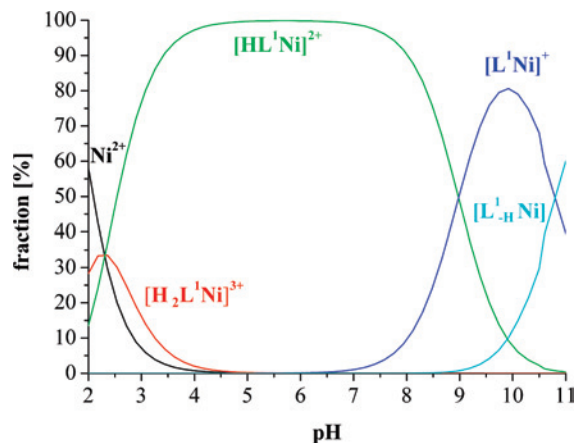
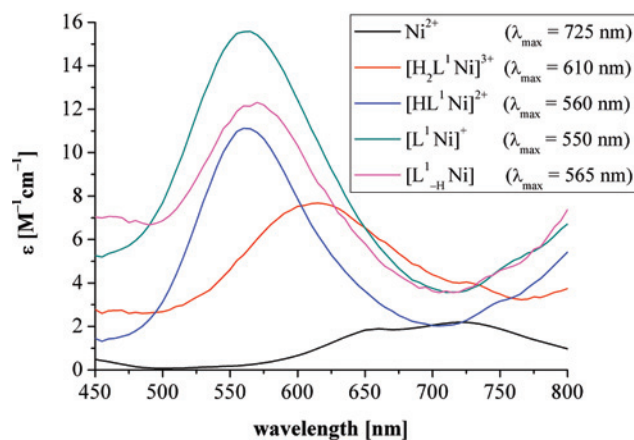
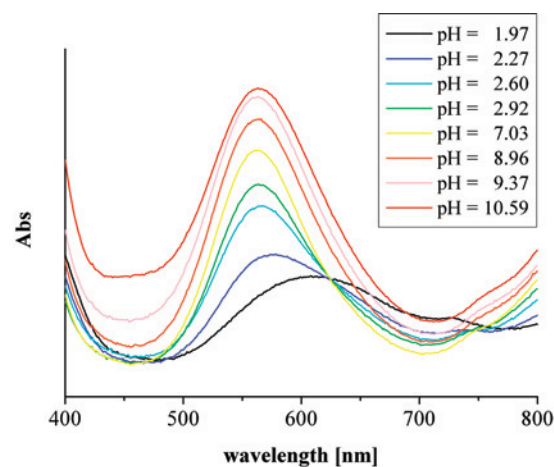
^a Standard deviations are given in parenthesis.**Table 3.** Overall Stability Constants ($\log \beta$) and Dissociation Constants (pK) for the Complexes formed with Zn^{2+} at 25 °C with $I = 0.2$ M (KCl)^a

	$[H_3L^1Zn]^{4+}$	$[H_2L^1Zn]^{3+}$	$[HL^1Zn]^{2+}$	$[L^1Zn]^+$
$\log \beta$	13.26(7)	9.82(9)	6.51(3)	-0.24(6)
pK	3.44	3.31	6.75	

^a Standard deviations are given in parenthesis.**Figure 1.** Concentration distribution of the species formed between HL^1 and Zn^{2+} at a 1:1 ligand to metal ratio. $c_{HL^1} = 1.7 \times 10^{-3}$ M.

mononuclear. These two species are observable up to pH 5, while the new species $[HL^1Zn]^{2+}$ is formed from around pH 3 and becomes almost the sole species at pH 5 (Figure 1). $[HL^1Zn]^{2+}$ likely contains a nondeprotonated pyrazole ring where the zinc ion is ligated by the appended imidazole heterocycles only (plus water). At more basic conditions further deprotonation takes place and another species $[L^1Zn]^+$ is observed. In view of the high bridging tendency of deprotonated pyrazolate, this species most likely features a bis(pyrazolato) bridged dizinc core with the formula $[L^1_2Zn_2]^{2+}$. Note that by pH potentiometry one determines the ratio of the components (metal/ligand/proton), which does not allow differentiating between species with a 1:1 or 2:2 metal to ligand ratio.

The results of the titration of ligand HL^1 in the presence of one equivalent Ni^{2+} are shown in Figure 2. At pH 2, free Ni^{2+} and a species $[H_2L^1Ni]^{3+}$ are present, but from pH ~ 2.5 on, the very dominant species is $[HL^1Ni]^{2+}$. This complex, for which one may assume that the pyrazole still bears its NH proton, is almost the sole species over a wide pH range up to pH 7. If the pH increases to 9 the pyrazole-NH dissociates and the monocationic species $[L^1Ni]^+$ is formed. Different from the Zn^{2+} case, however, a further deprotonation step leads to neutral $[L^1_{-H}Ni]$ which becomes the major species under very basic conditions above pH 11. The calculated pK value of 10.82 for $[L^1Ni]^+$ should represent the acidity of a metal-bound water to give $[L^1_{-H}Ni]$, which is thus better described as $[L^1Ni(OH)]$.

**Figure 2.** Concentration distribution of the species formed between HL^1 and Ni^{2+} at a 1:1 ligand to metal ratio. $c_{HL^1} = 1.7 \times 10^{-3}$ M.**Figure 3.** UV-vis spectra of HL^1 with 1 equiv of $NiCl_2$ in H_2O ($c = 4.5 \times 10^{-3}$ M) at various pHs from 1.93 to 10.85 (top) and UV-vis spectra of individual species from spectral deconvolution (bottom).

For the Ni^{II} system the pH dependent formation of different species was also investigated by UV-vis spectroscopy. UV-vis spectra were recorded for aqueous solutions containing HL^1 and one equivalent $NiCl_2$ in the range of pH 1.93 to 10.85 (Figure 3, top). At low pH values an absorption maximum at around 610 nm can be observed, which vanishes at pH 2.5 when a new absorption occurs at 560 nm. This result correlates well with the species distribution, where the species $[HL^1Ni]^{2+}$ is the major species between pH 2.5 and 9. A very small shift of λ_{max} to 550 nm can be detected at

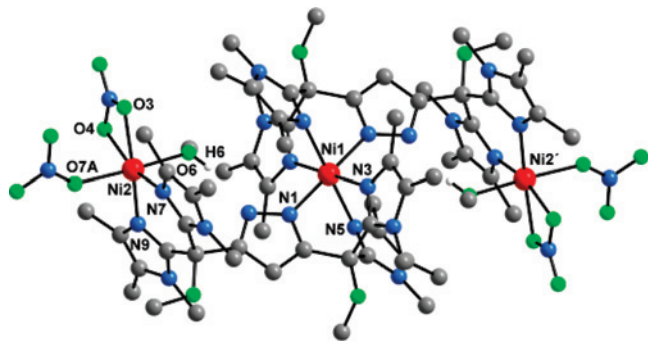


Figure 4. Molecular structure and numbering scheme of the cation of **4**. All hydrogen atoms except the O–H protons are not shown for clarity. Selected atom distances (Å) and angles (deg): Ni1–N1 = 2.033(4), Ni1–N3 = 2.144(4), Ni1–N5 = 2.138(4), Ni2–O3 = 2.115(3), Ni2–O4 = 2.153(4), Ni2–O6 = 2.120(3), Ni2–O7A = 2.095(4), Ni2–N7 = 2.018(4), Ni2–N9 = 2.009(4), Ni1···Ni2 = 6.6565(7), Ni2···Ni2' = 13.313(1), O6···N2 = 2.809(5); N1'–Ni1–N1 = 180.000(1), N3'–Ni1–N3 = 180.0, N5'–Ni1–N5 = 180.000(1), N1–Ni1–N3 = 85.94(14), N1'–Ni1–N3 = 94.06(14), N1–Ni1–N5 = 84.95(14), N1'–Ni1–N5 = 95.05(14), N3–Ni1–N5 = 86.77(14), N3'–Ni1–N5 = 93.23(14), N9–Ni2–N7 = 91.27(15), N9–Ni2–O3 = 166.17(15), N9–Ni2–O4 = 105.78(15), N9–Ni2–O6 = 87.70(14), N9–Ni2–O7A = 91.48(17), N7–Ni2–O3 = 102.14(15), N7–Ni2–O4 = 162.57(15), N7–Ni2–O6 = 90.95(14), N7–Ni2–O7A = 96.12(17), O7A–Ni2–O6 = 172.90(16), O6–H6···N2 162(9). Symmetry transformation used to generate equivalent atoms ('): 1 – x, 1 – y, 1 – z.

pH values around 10, suggesting that changes of the coordination around Ni²⁺ are only minor in that regime. Above pH 10 a slight red-shift to about 565 nm occurs, in accordance with the proposed formation of a hydroxo ligand in [L¹–_HNi]. Spectral deconvolution gives the λ_{max} values and molar absorptivities of the individual species, starting from Ni²⁺ (λ_{max} ca. 725 nm, with a shoulder at ca. 650 nm)¹⁸ at low pH to [L¹–_HNi] at highest pH (Figure 3, bottom). Low absorptivities for the Laporte forbidden d–d transitions are characteristic of octahedral Ni^{II}, and λ_{max} at about 540–550 nm for the ³A₂ → ³T₁(F) band is indicative of a {NiN₆} chromophore (depending on the number of chelate rings).¹⁸ One might therefore propose that in [L¹Ni]⁺ the Ni^{II} ion is bound to two facially tridentate donor caps each consisting of two imidazole-N and a pyrazolate-N; hence, this species would represent a binuclear bis(pyrazolato) bridged core with the formula [L₂Ni₂]²⁺, similar to the zinc case.

Structural and Spectroscopic Characterization of Ni^{II} Complexes. Crystalline material could be obtained for complexes of the fully methylated ligand HL² with Ni²⁺ and either nitrate or chloride as coligand, using vapor diffusion of diethyl ether into methanolic solutions of mixtures of the ligands and the respective metal salts. Molecular structures of complexes [L₂Ni₃(NO₃)₄(MeOH)₂] (**4**) and [L₂Ni₃Cl₂(MeOH)₄]Cl₂ (**5**) in the solid state were determined crystallographically, revealing the presence of unusual trinuclear species with ligand to metal ratio 2:3, irrespective of the ligand to metal ratio in the reaction mixtures (1:1 or 1:2) and the metal salt used (nitrate or chloride; Figures 4 and 5).

In both **4** and **5** a central Ni^{II} ion is found in an octahedral environment, composed of two facially disposed {N₃} donor

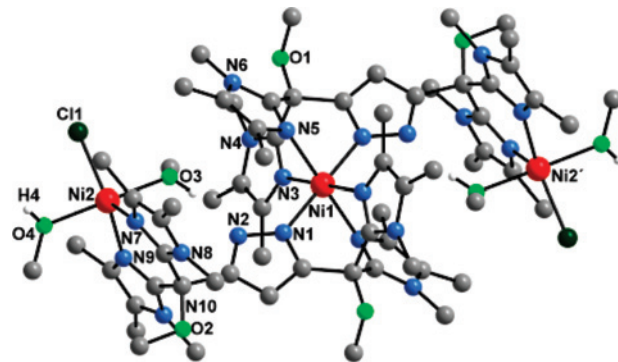
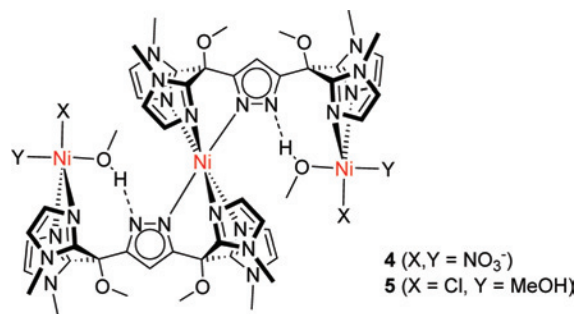


Figure 5. Molecular structure and numbering scheme of the cation of **5**. All hydrogen atoms except the O–H protons are not shown for clarity. Selected atom distances (Å) and angles (deg): Ni1–N1 = 2.026(4), Ni1–N3 = 2.138(4), Ni1–N5 = 2.133(4), Ni2–O3 = 2.103(3), Ni2–O4 = 2.078(4), Ni2–N7 = 1.999(4), Ni2–N9 = 1.993(4), Ni2–Cl1 = 2.2700(14), Ni1···Ni2 = 6.5676(8), Ni2···Ni2' = 13.135(2), O3···N2 = 2.765(5), O4···Cl2 = 3.034(5); N1'–Ni1–N1 = 180.000(1), N3'–Ni1–N3 = 180.000(1), N5'–Ni1–N5 = 180.0(2), N1–Ni1–N3 = 86.05(15), N1'–Ni1–N3 = 93.95(15), N1–Ni1–N5 = 84.61(15), N1'–Ni1–N5 = 95.39(15), N3–Ni1–N5 = 87.14(15), N3'–Ni1–N5 = 92.86(15), N9–Ni2–N7 = 90.58(16), N9–Ni2–Cl1 = 145.29(12), N9–Ni2–O3 = 86.24(15), N9–Ni2–O4 = 89.25(17), N7–Ni2–Cl1 = 123.29(12), N7–Ni2–O3 = 90.70(14), N7–Ni2–O4 = 96.83(16), O3–Ni2–Cl1 = 89.65(10), O4–Ni2–Cl1 = 89.81(12), O4–Ni2–O3 = 171.27(16), O3–H3···N2 169(6), O4–H4···Cl2 161(5). Symmetry transformation used to generate equivalent atoms ('): 1 – x, 1 – y, 1 – z.

Scheme 5. Schematic Representation of the Trinuclear Structure of Ni^{II}-Complexes **4** and **5**^a



^a Methyl substituents at the imidazole-C atoms are omitted for clarity.

sets from two different ligands [L²]⁻. Ni–N^{pz} bonds (2.033(4) and 2.026(4) Å) are somewhat longer than Ni–N^{im} bonds (1.993(4)–2.018(4) Å), although the reverse situation could have been expected because of the anionic charge of the pyrazolate. The outer Ni^{II} ions, however, are bound only to the appended imidazole groups while a methanol molecule has been inserted between those Ni and the N^{pz} atoms to form a strong intramolecular O–H···N^{pz} hydrogen bond (*d*(O···N) = 2.809(5) and 2.765(5) Å; Scheme 5). This leads to rather large Ni···Ni separations of around 6.6 Å. Two nitrate ions (in the case of **4**; one nitrate is bidentate) or a chloride and an additional methanol (in the case of **5**) complete the coordination spheres of those outer Ni^{II} ions. While each pyrazolate-based ligand scaffold indeed exhibits the anticipated tripodal tridentate coordination mode toward the central metal ion, the situation at the outer Ni^{II} illustrates that the coordination behavior may be more complex than expected. Unfortunately, no crystalline Zn^{II} complexes of ligands HL¹–HL³ could be isolated so far.

(18) *Spectroscopy and Structure of Metal Chelate Compounds*; Nakamoto, K., McCarthy, P. J., Eds.; John Wiley and Sons: New York, 1968.

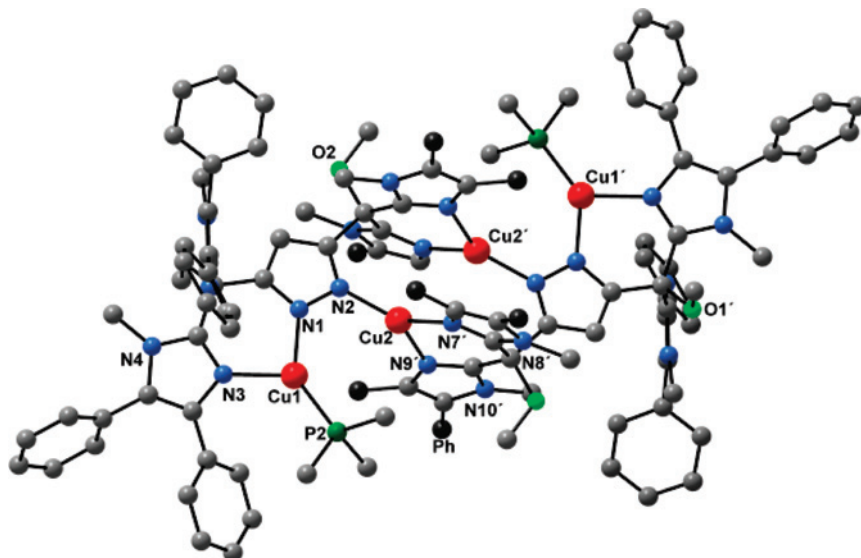


Figure 6. Molecular structure and numbering scheme of the cation of **6**. The inner phenyl groups of the imidazole rings and all hydrogen atoms are not shown for clarity. Selected atom distances (Å) and angles (deg): Cu1–N1 = 1.972(4), Cu1–N3 = 2.050(4), Cu1–P2 = 2.1759(16), Cu2–N2 = 1.934(4), Cu2–N7' = 1.998(4), Cu2–N9' = 2.012(4), Cu1...Cu2 = 3.505(1), Cu2...Cu2' = 3.325(1); N1–Cu1–N3 = 91.54(16), N1–Cu1–P2 = 140.19(12), N3–Cu1–P2 = 127.70(13), N2–Cu2–N7' = 133.97(16), N2–Cu2–N9' = 131.63(16), N7'–Cu2–N9' = 94.41(16). Symmetry transformation used to generate equivalent atoms (\prime): $1 - x, 1 - y, 1 - z$.

Besides the intense $\pi \rightarrow \pi^*$ and charge transfer (CT) bands at < 300 nm, the UV–vis spectrum of **5** in MeCN shows weak ligand field bands at 426 nm ($\epsilon = 151 \text{ M}^{-1} \cdot \text{cm}^{-1}$) and 726 nm ($\epsilon = 44$), in accordance with the presence of high-spin nickel(II) ions.¹⁹ These features are very similar to those observed for a solid sample (diffuse reflectance, $\lambda_{\text{max}} = 242, 415, 706$ nm), suggesting that the trinuclear entities remain intact in solution.

Once crystallized from MeOH/diethyl ether, complex **4** is only sparingly soluble in MeOH; hence, its UV–vis spectrum has been measured in dmf solution, showing a weak broad band at 639 nm ($\epsilon = 32$). A similar band position for the d–d transition is observed in the solid state (644 nm; additional high energy bands at 345 and 245 nm). It thus appears that even coordinating solvents such as dmf do not cause degradation of the trimetallic entities in solution. This is in line with the electrospray ionization mass spectrometry (ESI-MS) spectra of a dilute MeOH solution of **4**, which show prominent peaks at m/z 1534.5 and 736.4 with isotopic distribution patterns characteristic for the ions $[\text{L}_2^2\text{Ni}_3(\text{NO}_3)_3]^+$ and $[\text{L}_2^2\text{Ni}_3(\text{NO}_3)_2]^{2+}$, respectively. Assignment of the latter was further confirmed by a high-resolution (HR) ESI mass spectrum (see Experimental Section).

Structural and Spectroscopic Characterization of Cu^I complexes. Cu^I complexes were prepared by deprotonation of the respective ligand with one equivalent of KO^{*t*}Bu in the presence of two equivalents of $[\text{Cu}(\text{MeCN})_4]\text{PF}_6$, all carried out in THF or MeCN solutions under anaerobic conditions in a glovebox. Because no homogeneous compound could be isolated from those reaction mixtures, two equivalents of an additional coligand were then added and the products crystallized by vapor diffusion of diethyl ether

into CH_2Cl_2 solutions of the complexes. Crystalline material suitable for X-ray diffractometry could be obtained from HL^3 and PMe_3 or different isocyanides as coligands. While all complexes have the anticipated ligand to metal ratio 1:2, dimerization of two bimetallic entities is observed, giving rise to unusual tetrametallic complexes. Molecular structures of $[\text{L}_2^2\text{Cu}_4(\text{PMe}_3)_2](\text{PF}_6)_2$ (**6**) and $[\text{L}_2^2\text{Cu}_4(\text{CN}n\text{Bu})_2](\text{PF}_6)_2$ (**7**) are depicted in Figures 6 and 7, and the structure of $[\text{L}_2^2\text{Cu}_4(\text{CNC}_6\text{H}_3\text{Me}_2-2,6)_2](\text{PF}_6)_2$ (**8**) is shown in the Supporting Information, Figure S4.

All three complexes **6–8** adopt very similar structures. They consist of four metal ions in a roughly linear arrangement but with different coligands (PMe_3 or isocyanides) bound to the two outer metal ions. Both pyrazolate scaffolds act as bridging ligands that span a pair of Cu^I ions (Scheme 6). All Cu^I ions are three-coordinate in a distorted trigonal-planar arrangement; the two inner metals are bound to two imidazole-N from one ligand sidearm and a pyrazolate-N from the other ligand while the outer Cu^I ions are hosted by the pyrazolate-N and one imidazole-N from the nearby sidearm, forming a six-membered $\{\text{N}_2\}$ chelate, with the third coordination site filled by the coligand. The remaining imidazole ring at the periphery remains uncoordinated and dangling. Because of the very acute N1–Cu1–N3 angles of $91.5(2)^\circ$ (**6**), $92.7(1)^\circ$ (**7**), or $92.0(1)^\circ$ (**8**), both N–Cu1–L angles (L = donor atom of the coligand) are much larger than 120° (values $127.7(1)/140.2(1)^\circ$ for **6**, $128.1(1)/139.2(1)^\circ$ for **7**, $131.3(1)/136.6(1)^\circ$ for **8**).

The distance between the two inner copper ions is quite short (3.32 \AA for **6**, 3.27 \AA for **7**, 3.29 \AA for **8**), while the distance between copper ions bridged by the pyrazolate is somewhat larger at 3.50 \AA for **6** and 3.37 \AA for **7** but almost equal at 3.28 \AA for **8**. These latter values are still quite small when compared to other bimetallic systems of pyrazolates

(19) Meyer, F.; Kozłowski, H. In *Comprehensive Coordination Chemistry II*; McCleverty, J. A., Meyer, T. J., Eds.; Elsevier: Oxford, U.K., 2004; Vol. 6, pp 247–554.

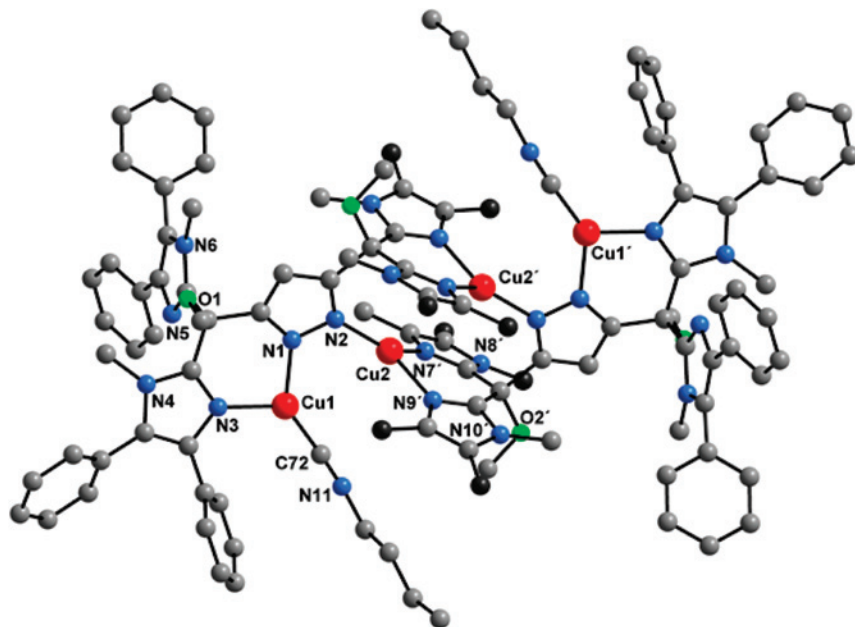
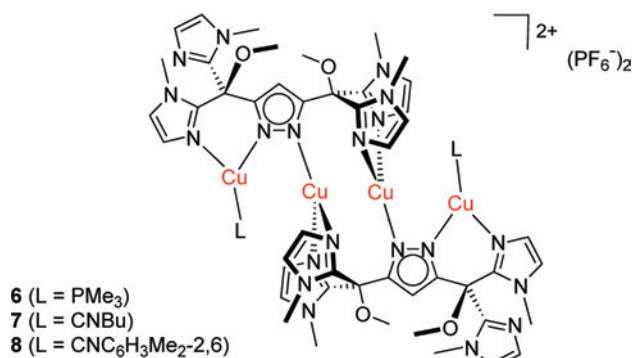


Figure 7. Molecular structure and numbering scheme of the cation of **7**. The inner phenyl groups of the imidazole rings and all hydrogen atoms are not shown for clarity. Selected atom distances (Å) and angles (deg): Cu1–N1 = 1.942(3), Cu1–N3 = 2.001(3), Cu1–C72 = 1.823(4), Cu2–N2 = 1.927(3), Cu2–N7' = 2.002(3), Cu2–N9' = 2.024(3), Cu1...Cu2 = 3.3656(6), Cu2...Cu2' = 3.2742(8); N1–Cu1–N3 = 92.71(11), N1–Cu1–C72 = 139.21(14), N3–Cu1–C72 = 128.05(14), N2–Cu2–N7' = 135.66(11), N2–Cu2–N9' = 132.31(11), N7'–Cu2–N9' = 92.00(11). Symmetry transformation used to generate equivalent atoms ('): 1 – x, 1 – y, 1 – z.

Scheme 6. Schematic Representation of the Tetranuclear Structure of Cu^I Complexes **6**, **7**, and **8**^a



^a Phenyl substituents at the imidazole-C atoms are omitted for clarity.

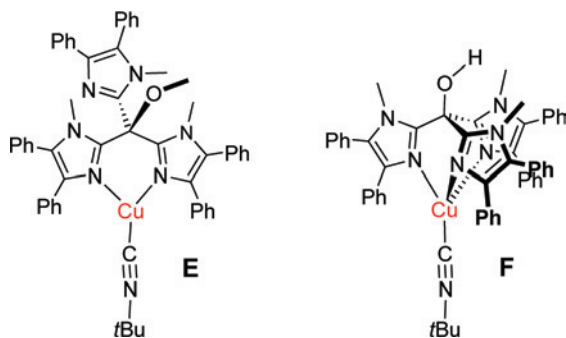
with appended chelate arms.^{3,4,20} This may be the reason for the metal ions in **6–8** to displace out of the plane of the pyrazolate (evidenced by the torsion angles Cu1–N1–N2–Cu2 of 7.4(5)° (**6**), 15.5(3)° (**7**), and 8.0(2)° (**8**)). All Cu–N bonds are found in the usual range with Cu–N^{im} around 2.0 Å, and Cu–N^{pz} slightly shorter at 1.91–1.97 Å because of the negative charge on the pyrazolate. Distances between the outer Cu^I ions and the isocyanide-C in complexes **7** and **8** are 1.818(2) and 1.823(4) Å, respectively, which is quite short in comparison to other three-coordinate Cu^I compounds with bound isocyanide ligands.²¹ However, IR absorptions for the ν(C≡N) stretches (2196 cm⁻¹ for **7**, 2155 cm⁻¹ for **8**) are in the usual range, that is, slightly shifted to higher energy compared to the free isocyanides (2149 cm⁻¹ for CN*n*Bu, 2121

cm⁻¹ for CNC₆H₃Me₂-2,6).²² This is often observed when the terminally bound isocyanides act as σ-donors toward Cu^I with only little π-backbonding.^{23,24}

ESI mass spectra of the isolated complexes in MeCN solution are basically identical to spectra of the crude reaction mixtures before crystallization. In all cases, the peak of highest *m/z* corresponds to the ions [L³Cu₂L₂]⁺ (confirmed by high-resolution MS) while no signal is detected for the tetranuclear species that have been found in the solid state. Further peaks are observed for, inter alia, [L³Cu₂L]⁺ and [L³Cu]⁺, the latter one being the most intensive in all spectra. A high-resolution mass spectrum of **8** reveals an additional minor peak at *m/z* = 1340.41943 that according to its isotopic distribution pattern stems from the ion [L³₂Cu₄(C₆H₃Me₂-2,6)₂]²⁺. These findings suggest that the tetranuclear species may indeed exist in solution, but most likely they are partly dissociated into their bimetallic constituents. ¹H and ¹³C NMR spectroscopy confirms the presence of several species in solution, some of which have nonequivalent N^{im}Me and OMe groups, in accordance with some aggregation of the bimetallic {L³Cu₂} building blocks.

- (21) (a) Ardizzoia, G. A.; Cenini, S.; La Monica, G.; Masciocchi, N.; Maspero, A.; Moret, M. *Inorg. Chem.* **1998**, *37*, 4284–4292. (b) Badiei, Y. M.; Warren, T. H. *J. Organomet. Chem.* **2005**, *690*, 5989–6000. (c) Ardizzoia, G. A.; Beccalli, E. M.; La Monica, G.; Masciocchi, N.; Moret, M. *Inorg. Chem.* **1992**, *31*, 2706–2711. (d) Jazdzewski, B. A.; Holland, P. L.; Pink, M.; Young, V. G.; Spencer, D. J. E.; Tolman, W. B. *Inorg. Chem.* **2001**, *40*, 6097–6107.
- (22) Teichgräber, J.; Dechert, S.; Meyer, F. *J. Organomet. Chem.* **2005**, *690*, 5255–5263.
- (23) (a) Cotton, F. A.; Zingales, F. *J. Am. Chem. Soc.* **1961**, *83*, 351–355. (b) Tsuda, T.; Sanada, S.-I.; Ueda, K.; Saegusa, T. *Inorg. Chem.* **1976**, *15*, 2329–2332.
- (24) (a) Aryl isocyanides are better π-acceptors than alkyl isocyanides, Treichel, P. M. *Adv. Organomet. Chem.* **1973**, *11*, 21–86. (b) Singleton, E.; Oosthuizen, H. E. *Adv. Organomet. Chem.* **1983**, *22*, 209–310.

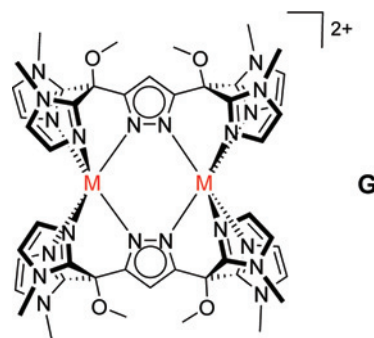
(20) Klingele, J.; Dechert, S.; Meyer, F. *Coord. Chem. Rev.*; submitted for publication.

Scheme 7. Mononuclear Cu^I–Isonitrile Complexes of Tripodal Tris(imidazolyl)methane Ligands¹³

Discussion and Conclusions

The new ligands HL¹–HL³ have been designed to provide two tripodal {N₃} donor compartments, predestined to accommodate two metal ions in close proximity. The anticipated binding mode is indeed realized for the central Ni^{II} ion of the trinuclear complexes **4** and **5**, but the situation for the outer metal ions in those Ni^{II} complexes, as well as our findings for the Cu^I complexes **6–8**, indicate that this facially tridentate binding mode is not particularly favored. Instead, the presence of competing ligands such as PMe₃ or isocyanides in the Cu case, or even the presence of counteranions or MeOH solvent molecules in the Ni case, may readily lead to dissociation of one of the N donor legs of the {N₃} compartment, leaving the pyrazolate-based ligand bidentate toward the respective metal ion—either 2 × N^{im} as observed for the outer Ni ions in **4** and **5** as well as for the central Cu ions in **6–8** or one N^{im} and one N^{pz} as observed for the outer Cu ions in **6–8**. It is interesting to note that a similar behavior has previously been found for the corresponding mononuclear systems based on tripodal tris(imidazolyl)methane ligands (compare **D**, Scheme 3). Nicholas and co-workers recently reported the molecular structures of complexes **E** and **F** derived from a tripodal ligand very reminiscent of the individual binding pockets of HL³, where either bidentate coordination with one dangling imidazole or tridentate coordination involving all three N^{im} was observed depending on whether the backbone methane substituent was an OMe group (**E**) or a free OH (**F**).¹³ Furthermore, a bridged arrangement identical to the metalocycle comprising the two inner Cu^I ions in **6–8** has been found for the same tris(imidazolyl)methane system in the absence of any coligand, and earlier by Sorrell and Borovik for a related carbinol ligand.¹⁰

The discrepancy regarding the nuclearity of species observed by pH potentiometry in aqueous solution and by X-ray crystallography in the solid state may, at least in part, be ascribed to the different ligand systems. The parent ligand HL¹ that was used in the titration experiments might give rise to species [L¹₂M₂]²⁺ with bis(pyrazolato) bridged bimetallic core (**G**, Scheme 8; related bis(pyrazolato) bridged structures where some of the imidazole side arms are noncoordinating are conceivable as well), whereas the more bulky backbone substituents at the imidazole rings of HL² and HL³ will prevent the formation of such compact structures. Unfortunately, crystalline material could only be

Scheme 8. Schematic Representation of the Binuclear Species That Is Assumed to Exist at Appropriate pH in Aqueous Solution for HL¹

obtained with HL² for Ni^{II} and with HL³ for Cu^I while the limited solubility of HL² and HL³ in aqueous media hampers their use in pH potentiometry. In the case of intermediate ligand steric bulk, that is, for backbone methyl groups in HL², the anticipated tripodal tridentate coordination mode and the formation of a {NiN₆} chromophore may still be realized if the opposite ligand strands are dislocated, as observed for the central metal ions in **4** and **5**. The even bulkier phenyl groups in HL³ should completely prevent such a situation, in accordance with the structures observed for **6–8**. In addition to these ligand steric requirements, discrepancies regarding the nuclearity of species observed by pH potentiometry in aqueous solution, by X-ray crystallography in the solid state, and by UV–vis and ESI-MS in organic solvents may likely result from the different coordinating strength and protolytic behavior of the solvents, again confirming that these ligands are rather flexible and are not suited to firmly impose a specific binding mode.

While the situation for the central Ni^{II} ions in **4** and **5** shows that an OMe group at the bridgehead C atom does not necessarily preclude the tripodal tridentate coordination mode for HL¹–HL³, a delicate energetic balance between the stereoelectronic characteristics of the particular {N₃} donor set, the preferences of the respective metal ion, and the possible steric crowding between the methine substituent (OMe or OH) and the imidazolyl NMe groups on the tripod backside may also contribute to the multifaceted coordination behavior of these systems.¹³ In any case it is pleasing to note that the coordination motifs found for the oligonuclear complexes **4–8** find their exact counterpart in the chemistry of related mononuclear complexes, which confirms our view that ligands HL¹–HL³ can be described as novel binucleating versions of the tripodal tris(imidazolyl)methanes. It will be interesting to probe their further coordination chemistry and the reactivity of their complexes in view of this analogy.

Experimental Section

General Procedures and Methods. Solvents were distilled from potassium (THF) or calcium hydride (dichloromethane) under an atmosphere of dry nitrogen. *N*-methylimidazole, methyl iodide, trimethylphosphine (1.0 M in THF), sodium hydride, *n*-butylisonitrile, 2,6-dimethylphenylisonitrile, *n*-butyllithium (1.6 M in *n*-hexane), and nickel(II)-salts were obtained from commercial sources

used without further purification. **1**¹⁶ and [Cu(MeCN)₄]PF₆,²⁵ 1,4,5-trimethylimidazole²⁶ and 1-methyl-4,5-diphenylimidazole²⁷ were prepared as described in the literature. The synthesis of all copper(I)-complexes were carried out in an MBRAUN Glove Box with integrated solvent purification system (SPS) under an atmosphere of dry nitrogen. ¹H and ¹³C NMR spectra were recorded at 298 K on Bruker Avance 300 or Avance 500 spectrometers, operating at 300 and 500 MHz (¹H), or 75 and 125 MHz (¹³C). ¹H and ¹³C NMR chemical shifts were referenced internally to residual solvent resonances (CDCl₃: δ_H = 7.24, δ_C = 77.0 ppm; DMSO: δ_H = 2.49, δ_C = 39.4 ppm; CD₃CN: δ_H = 1.94, δ_C = 1.3 ppm). IR spectra were recorded as KBr pellets using a Digilab Excalibur, and UV–vis spectra were measured on a Varian Cary 5000. Mass spectra were recorded with a Finnigan MAT 95 (FAB) using 3-nitrobenzylalcohol as matrix or with a Finnigan MAT 8200 (EI). ESI mass spectra were measured on an API 2000 MS/MS system for acetonitrile solutions. Elemental analyses were performed by the “Analytisches Labor des Instituts für Anorganische Chemie der Universität Göttingen” on an Elementar varioELIII. The melting- and decomposition points have been measured with an OptiMelt MPA 100 (Stanford Research Systems) at a heating rate of 5 K/min and are uncorrected.

Preparation of the Ligands. 3,5-Bis[bis(1-methyl-1H-imidazol-2-yl)hydroxymethyl]-1-tetrahydropyran-2-yl-1H-pyrazole (2a). *N*-butyllithium (1.6 M in *n*-hexane, 63 mL, 100 mmol) was added dropwise via syringe to a stirred solution of *N*-methylimidazole (8.0 mL, 8.21 g, 100 mmol) in dry THF (450 mL) over 30 min under N₂ at room temperature. The orange reaction mixture was stirred for additional 2 h, and a solution of **1** (6.70 g, 25 mmol) in dry THF (150 mL) was then added slowly over 15 min. Stirring was continued overnight at room temperature. Methanol (60 mL) was then added, which caused the color to turn from grayish-yellow to light yellow. All solvents were removed under reduced pressure and water (50 mL) added. The solution was extracted with chloroform (5 × 50 mL), and the aqueous phase evaporated to dryness. The residue was redissolved in chloroform (250 mL), and the solution dried over MgSO₄. After evaporation of the solvent, **2a** (6.38 g, 12 mmol, 48%) was obtained as a white solid.

MS (FAB⁺) *m/z* (relative intensity): 533 (52, [M + H]⁺), 451 (7, [M + H - Im]⁺), 449 (10, [M + H - thp]⁺), 367 (18, [M + H - thp - Im]⁺), 285 (100 [M + H - thp - 2Im]⁺), 83 (14, [Im + H]⁺). ¹H NMR (300 MHz, CDCl₃): δ 6.70–6.85 (m, 8H, H^{Im4} + 5), 5.79 (s, 1H, H^{Pz4}), 5.35 (dd, 1H, ³J = 9.6 Hz, ³J = 1.8 Hz, H^{Thp2}), 3.55–3.65 (m, 1H, H^{Thp3}), 3.54 (s, 3H, NCH₃), 3.37 (s, 3H, NCH₃), 3.35 (s, 3H, NCH₃), 3.27 (s, 3H, NCH₃), 3.00–3.20 (m, 1H, H^{Thp3}), 2.05–2.20 (m, 1H, H^{Thp6}), 1.70–1.90 (m, 2H, H^{Thp5} + 6), 1.35–1.50 (m, 2H, H^{Thp4} + 5), 1.25–1.35 (m, 1H, H^{Thp4}) ppm. ¹³C NMR (75 MHz, CDCl₃): δ 152.1 (C^{Pz5}), 147.3 (C^{Im2}), 147.1 (C^{Im2}), 146.6 (C^{Im2}), 146.2 (C^{Im2}), 142.8 (C^{Pz3}), 126.4 (C^{Im4}), 125.7 (C^{Im4}), 125.6 (C^{Im4}), 125.4 (C^{Im4}), 123.6 (C^{Im5}), 123.3 (C^{Im5}), 123.2 (C^{Im5}), 123.2 (C^{Im5}), 107.0 (C^{Pz4}), 85.0 (C^{Thp1}), 71.4 (COH), 70.1 (COH), 67.7 (C^{Thp3}), 34.6 (NCH₃), 34.4 (NCH₃), 34.2 (NCH₃), 34.1 (NCH₃), 29.2 (C^{Thp6}), 24.7 (C^{Thp4}), 22.6 (C^{Thp5}) ppm. IR (KBr, cm⁻¹): 3347 (br), 3109 (s), 3048 (m), 2949 (s), 2858 (s), 2736 (br), 1645 (m), 1525 (m), 1489 (vs), 1456 (s), 1404 (s), 1350 (s), 1320 (m), 1283 (vs), 1259 (m), 1205 (s), 1130 (s), 1084 (s), 1042 (s), 1007 (s), 948 (vs), 896 (s), 874 (s), 822 (m), 732 (br), 701 (m),

553 (w), 457 (w). mp: 130 °C (decomp.). Anal. Calcd for C₂₆H₃₂N₁₀O₃·(2THF + 0.5H₂O) (685.83): C, 59.54; H, 7.20; N, 20.42. Found: C, 59.63; H, 7.09; N, 20.43.

3,5-Bis[bis(1-methyl-1H-imidazol-2-yl)methoxymethyl]-1-tetrahydropyran-2-yl-1H-pyrazole (3a). A solution of **2a** (3.69 g, 6.9 mmol) in dry THF (50 mL) was added dropwise to a suspension of NaH (0.37 g, 15.3 mmol) in dry THF (200 mL) under N₂. The reaction mixture was stirred for 2 h, and methyl iodide (0.95 mL, 15.3 mmol) was then added via syringe. The resulting solution was stirred overnight at room temperature. Half-saturated NaCl solution (50 mL) was added, and THF was removed under reduced pressure. The resulting aqueous solution was extracted with chloroform (5 × 50 mL), the organic layer dried over MgSO₄, filtered, and the solvent removed under reduced pressure to give **3a** (3.32 g, 5.9 mmol, 86%) as a white solid.

MS (FAB⁺) *m/z* (relative intensity): 583 (40, [M + Na]⁺), 561 (100, [M + H]⁺), 547 (22, [M + H - CH₃]⁺), 477 (40, [M + H - thp]⁺), 349 (26, [M + H - thp - Im - OCH₃ - CH₃]⁺). ¹H NMR (500 MHz, CDCl₃): δ 6.80–7.00 (m, 8H, H^{Im4} + 5), 6.44 (s, 1H, H^{Pz4}), 5.49 (dd, 1H, ³J = 8.1 Hz, ³J = 1.8 Hz, H^{Thp2}), 3.60–3.70 (m, 1H, H^{Thp6}), 3.51 (s, 3H, NCH₃), 3.45 (s, 6H, NCH₃), 3.39 (s, 3H, NCH₃), 3.36 (s, 3H, OCH₃), 3.32 (s, 3H, OCH₃), 3.25–3.35 (m, 1H, H^{Thp6}), 2.10–2.20 (m, 1H, H^{Thp3}), 1.75–1.85 (m, 1H, H^{Thp4}), 1.60–1.70 (m, 1H, H^{Thp3}), 1.40–1.50 (m, 2H, H^{Thp4} + 5), 1.25–1.35 (m, 1H, H^{Thp5}) ppm. ¹³C NMR (125 MHz, CDCl₃): δ 149.5 (C^{Pz5}), 145.8 (C^{Im2}), 145.64 (C^{Im2}), 144.2 (C^{Im2}), 144.1 (C^{Im2}), 140.0 (C^{Pz3}), 126.8 (C^{Im4}), 126.7 (C^{Im4}), 126.6 (C^{Im4}), 126.5 (C^{Im4}), 123.8 (C^{Im5}), 123.8 (C^{Im5}), 123.2 (C^{Im5}), 123.1 (C^{Im5}), 108.8 (C^{Pz4}), 85.3 (C^{Thp2}), 78.5 (COCH₃), 77.2 (COCH₃), 67.4 (C^{Thp6}), 54.2 (OCH₃), 53.8 (OCH₃), 34.7 (NCH₃), 34.7 (NCH₃), 34.6 (NCH₃), 34.5 (NCH₃), 29.6 (C^{Thp3}), 24.9 (C^{Thp5}), 22.9 (C^{Thp4}) ppm. IR (KBr, cm⁻¹): 3393 (br), 3107 (s), 2943 (vs), 2858 (s), 2576 (w), 2486 (w), 2187 (w), 2031 (w), 1905 (w), 1677 (m), 1638 (m), 1522 (m), 1485 (s), 1403 (s), 1354 (m), 1319 (m), 1282 (s), 1251 (m), 1206 (s), 1181 (m), 1132 (s), 1082 (br), 1031 (s), 1007 (s), 969 (s), 940 (m), 907 (s), 873 (s), 821 (m), 747 (br), 661 (m), 593 (w), 551 (w), 460 (w). mp: 121 °C (decomp.). Anal. Calcd for C₂₈H₃₆N₁₀O₃·(1.3CH₂Cl₂) (671.08): C, 52.44; H, 5.80; N, 20.87. Found: C, 52.57; H, 6.00; N, 20.68.

3,5-Bis[bis(1-methyl-1H-imidazol-2-yl)methoxymethyl]-1H-pyrazole hydrochloride (HL¹·HCl). A solution of **3** (14.66 g, 26.2 mmol) in ethanolic HCl (100 mL) was stirred overnight. Diethyl ether (Et₂O, 400 mL) was added, and the grayish precipitate was collected by filtration, washed with cold Et₂O, and dried in vacuo to give **HL¹·HCl** (14.02 g, 25.5 mmol, 98%) as a light gray solid.

MS (FAB⁺) *m/z* (relative intensity): 477 (100, [M - Cl]⁺), 463 (16, [M - Cl - CH₃]⁺), 413 (7, [M - Cl - 2OCH₃]⁺), 349 (9, [M - Cl - CH₃ - Im]⁺). ¹H NMR (500 MHz, DMSO): δ 7.73 (d, 4H, ³J = 1.6 Hz, H^{Im4}), 7.48 (d, 4H, ³J = 1.6 Hz, H^{Im5}), 6.89 (s, 1H, H^{Pz4}), 3.53 (s, 12H, NCH₃), 3.23 (s, 6H, OCH₃) ppm. ¹³C NMR (125 MHz, DMSO): δ 140.1 (C^{Im2}), 126.5 (C^{Im4/5}), 121.7 (C^{Im4/5}), 108.7 (C^{Pz4}), 74.8 (COCH₃), 53.3 (OCH₃), 35.3 (NCH₃) ppm. IR (KBr, cm⁻¹): 3400 (br), 3322 (br), 3118 (br), 2836 (br), 2734 (br), 1648 (m), 1590 (s), 1525 (s), 1454 (m), 1382 (s), 1321 (s), 1294 (s), 1206 (m), 1130 (m), 1087 (s), 1038 (m), 966 (m), 941 (m), 893 (m), 855 (m), 774 (s), 714 (m), 678 (m), 567 (m), 532 (m). mp: 163 °C (decomp.). Anal. Calcd for C₂₃H₂₉ClN₁₀O₂·(4.3HCl) (669.79): C, 41.24; H, 5.01; N, 20.91. Found: C, 41.41; H, 5.31; N, 20.72.

3,5-Bis[bis(1-methyl-1H-imidazol-2-yl)methoxymethyl]-1H-pyrazole (HL¹). The hydrochloride **HL¹·HCl** (14.02 g, 25.5 mmol) was dissolved in ammoniacal CH₂Cl₂ (100 mL), and the solution

(25) Kubas, G. J. *Inorg. Synth.* **1990**, 28, 68–69.

(26) Graf, F. Hupfer, L. DE 29 40 709 A1, 1981.

(27) Benisvy, L. Private communication, MPI Mülheim, 2004.

was stirred overnight. A fine precipitate was filtered off, the organic phase dried over MgSO_4 and evaporated to dryness. The light yellow crude product was purified by Soxhlet-extraction with diethyl ether. After the solvent was removed, **5** (5.92 g, 12.3 mmol, 48%) was obtained as a white solid.

MS (EI) m/z (relative intensity): 476 (5, $[\text{M}]^+$), 461 (38, $[\text{M} - \text{CH}_3]^+$), 446 (48, $[\text{M} - 2\text{CH}_3]^+$), 429 (32, $[\text{M} - \text{CH}_3 - \text{OCH}_3]^+$), 413 (5, $[\text{M} - 2\text{OCH}_3]^+$), 365 (6, $[\text{M} - \text{OCH}_3 - \text{Im}]^+$), 83 (100, $[\text{Im}]^+$). ^1H NMR (500 MHz, CDCl_3): δ 6.89 (d, 4H, $^3J = 1.2$ Hz, $\text{H}^{\text{Im}4}$), 6.77 (d, 4H, $^3J = 1.2$ Hz, $\text{H}^{\text{Im}5}$), 6.29 (s, 1H, $\text{H}^{\text{Pz}4}$), 3.35 (s, 12H, NCH_3), 3.15 (s, 6H, OCH_3) ppm. ^{13}C NMR (125 MHz, CDCl_3): δ 145.0 ($\text{C}^{\text{Im}2}$), 126.3 ($\text{C}^{\text{Im}4}$), 123.0 ($\text{C}^{\text{Im}5}$), 106.3 ($\text{C}^{\text{Pz}4}$), 77.2 (COCH_3), 52.4 (OCH_3), 33.9 (NCH_3) ppm. IR (KBr, cm^{-1}): 3104 (s), 2950 (s), 2827 (s), 1636 (w), 1522 (m), 1486 (vs), 1403 (s), 1347 (m), 1281 (vs), 1229 (m), 1186 (m), 1128 (s), 1074 (vs), 1013 (m), 970 (s), 907 (m), 892 (s), 819 (w), 752 (m), 729 (m), 685 (m), 558 (w), 464 (w). Anal. Calcd for $\text{C}_{23}\text{H}_{28}\text{N}_{10}\text{O}_2 \cdot 0.4\text{H}_2\text{O}$ (483.75): C, 57.11; H, 6.00; N, 28.95. Found: C, 57.44; H, 6.18; N, 28.70.

3,5-Bis-[bis-(1-Methylimidazol-2-yl)-hydroxymethyl]pyrazole hydrochloride ($\text{H}_3\text{L}^4 \cdot \text{HCl}$). A solution of **2a** (19.60 g, 36.8 mmol) in ethanolic HCl (150 mL) was stirred overnight. Et_2O (500 mL) was added to give a white precipitate that was collected by filtration, washed with cold Et_2O , and dried in vacuo to yield $\text{H}_3\text{L}^4 \cdot \text{HCl}$ (17.80 g, 36.7 mmol, 99%) as a white solid.

MS (FAB⁺) m/z (relative intensity): 449 (100, $[\text{M} - \text{Cl}]^+$), 367 (18, $[\text{M} - \text{Cl} - \text{Im}]^+$), 285 (45, $[\text{M} - \text{Cl} - 2\text{Im}]^+$), 83 (38, $[\text{Im} + \text{H}]^+$). ^1H NMR (500 MHz, DMSO): δ 7.83 (d, 4H, $^3J = 1.7$ Hz, $\text{H}^{\text{Im}4}$), 7.53 (d, 4H, $^3J = 1.7$ Hz, $\text{H}^{\text{Im}5}$), 6.73 (s, 1H, $\text{H}^{\text{Pz}4}$), 3.68 (s, 12H, NCH_3) ppm. ^{13}C NMR (125 MHz, DMSO): δ 145.1 ($\text{C}^{\text{Pz}3} + 5$), 141.6 ($\text{C}^{\text{Im}2}$), 126.7 ($\text{C}^{\text{Im}4}$), 120.1 ($\text{C}^{\text{Im}5}$), 106.5 ($\text{C}^{\text{Pz}4}$), 69.0 (COCH_3), 36.1 (NCH_3) ppm. IR (KBr, cm^{-1}): 3392 (br), 3118 (s), 3047 (s), 2966 (s), 2819 (s), 2741 (s), 1723 (w), 1639 (w), 1591 (m), 1520 (s), 1455 (m), 1384 (s), 1312 (s), 1279 (m), 1210 (m), 1161 (w), 1118 (m), 1072 (s), 1016 (w), 924 (m), 885 (m), 769 (s), 720 (m), 621 (w). mp: 180 °C (decomp.). Anal. Calcd for $\text{C}_{21}\text{H}_{25}\text{ClN}_{10}\text{O}_2 \cdot (3.9\text{HCl} + 0.4\text{EtOH})$ (643.75): C, 40.55; H, 4.90; N, 21.69. Found: C, 40.55; H, 5.35; N, 21.82.

3,5-Bis[bis(1-methyl-1H-imidazol-2-yl)hydroxymethyl]-1H-pyrazole (H_3L^4). The hydrochloride $\text{H}_3\text{L}^4 \cdot \text{HCl}$ (17.80 g, 36.7 mmol) was dissolved in ammoniacal CH_2Cl_2 (250 mL), and the solution was stirred for 3 h. A fine precipitate was filtered off, and the organic phase dried over MgSO_4 . After the solvent was removed, **5** (3.38 g, 7.6 mmol, 21%) was obtained as a white solid.

MS (EI) m/z (relative intensity): 448 (1, $[\text{M}]^+$), 366 (4, $[\text{M} - \text{Im}]^+$), 285 (4, $[\text{M} - 2\text{Im}]^+$), 82 (100, $[\text{Im}]^+$). ^1H NMR (500 MHz, DMSO): δ 12.52 (br, 1H, NH), 7.11 (s, 4H, $\text{H}^{\text{Im}4}$), 6.73 (s, 4H, $\text{H}^{\text{Im}5}$), 5.80 (s, 1H, $\text{H}^{\text{Pz}4}$), 3.39 (s, 12H, NCH_3) ppm. ^{13}C NMR (125 MHz, DMSO): δ 147.59 ($\text{C}^{\text{Pz}3} + 5$), 125.02 ($\text{C}^{\text{Im}4}$), 123.62 ($\text{C}^{\text{Im}5}$), 103.59 ($\text{C}^{\text{Pz}4}$), 70.93 (COH), 33.93 (NCH_3) ppm. IR (KBr, cm^{-1}): 3133 (s), 3046 (s), 2824 (m), 1755 (w), 1690 (w), 1618 (w), 1530 (w), 1486 (s), 1447 (m), 1403 (vs), 1282 (s), 1196 (m), 1129 (m), 1038 (m), 937 (m), 898 (s), 818 (w), 757 (m), 723 (w), 682 (w), 551 (w), 448 (w). mp: 154 °C (decomp.).

3,5-Bis-[bis-(1,4,5-trimethylimidazol-2-yl)-hydroxymethyl]-1-tetrahydropyran-2-yl-pyrazole (2b**)**. At room temperature and under nitrogen, freshly sublimed 1,4,5-trimethylimidazole (11.00 g, 100.0 mmol) was dissolved in dry THF (450 mL). *n*-Butyllithium (63 mL, 100.8 mmol, 1.6 M in *n*-hexane) was added, and the resulting orange solution stirred for 1 h. A solution of **1** (6.70 g, 25.0 mmol) in dry THF (150 mL) was added, and the red suspension stirred overnight at room temperature. The reaction mixture was then quenched with half-saturated ammonium chloride solution (90

mL), and the solvents were removed under reduced pressure. The yellow crude product was redissolved in ammoniacal CH_2Cl_2 (250 mL), filtered, and dried over MgSO_4 . After evaporation of the solvent in vacuum, **2b** was obtained as a white solid (13.98 g, 21.7 mmol, 87%).

MS (FAB⁺) m/z (relative intensity): 645 (93, $[\text{M} + \text{H}]^+$), 535 (12, $[\text{M} + \text{H} - \text{Tri}]^+$), 341 (100, $[\text{M} + \text{H} - 2\text{Tri} - \text{thp}]^+$), 247 (7, $[\text{C}(\text{OH})(\text{Tri})_2]^+$), 111 (42, $[\text{Tri} + \text{H}]^+$). ^1H NMR (CDCl_3): δ 6.40 (br, 1H, OH), 5.88 (s, 1H, $\text{H}^{\text{Pz}4}$), 5.85 (br, 1H, OH), 5.32 (dd, 1H, $\text{H}^{\text{Thp}2}$, $^3J = 2.2$ Hz, $^3J = 10.0$ Hz), 3.55–3.65 (m, 1H, $\text{H}^{\text{Thp}6}$), 3.40 (s, 3H, NCH_3), 3.26 (s, 3H, NCH_3), 3.18 (s, 3H, NCH_3), 3.13 (s, 4H, $\text{NCH}_3 + \text{H}^{\text{Thp}6}$), 2.10–2.20 (m, 1H, $\text{H}^{\text{Thp}3}$), 2.00–2.10 (m, 24H, CCH_3), 1.75–1.90 (m, 1H, $\text{H}^{\text{Thp}4}$), 1.65–1.75 (m, 1H, $\text{H}^{\text{Thp}3}$), 1.25–1.55 (m, 3H, $\text{H}^{\text{Thp}4} + 5$) ppm. ^{13}C NMR (CDCl_3): δ 152.7 ($\text{C}^{\text{Pz}5}$), 145.0 ($\text{C}^{\text{Im}2}$), 144.8 ($\text{C}^{\text{Im}2}$), 144.4 ($\text{C}^{\text{Im}2}$), 143.9 ($\text{C}^{\text{Im}2}$), 142.8 ($\text{C}^{\text{Pz}3}$), 130.9 ($\text{C}^{\text{Im}4}$), 130.2 ($\text{C}^{\text{Im}4}$), 130.0 ($\text{C}^{\text{Im}4}$), 129.9 ($\text{C}^{\text{Im}4}$), 125.2 ($\text{C}^{\text{Im}5}$), 124.9 ($\text{C}^{\text{Im}5}$), 124.8 ($\text{C}^{\text{Im}5}$), 124.7 ($\text{C}^{\text{Im}5}$), 107.5 ($\text{C}^{\text{Pz}4}$), 84.7 ($\text{C}^{\text{Thp}2}$), 71.0 (COH), 69.8 (COH), 67.4 ($\text{C}^{\text{Thp}6}$), 31.8 (NCH_3), 31.5 (NCH_3), 31.4 (NCH_3), 31.4 (NCH_3), 29.1 ($\text{C}^{\text{Thp}3}$), 24.7 ($\text{C}^{\text{Thp}5}$), 22.7 ($\text{C}^{\text{Thp}4}$), 12.5 (CCH_3), 12.4 (CCH_3), 12.4 (CCH_3), 12.3 (CCH_3), 8.8 (CCH_3), 8.8 (CCH_3), 8.7 (CCH_3), 8.7 (CCH_3) ppm. ^1H NMR (DMSO): δ 7.00 (br, 1H, OH), 6.30 (br, 1H, OH), 6.06 (s, 1H, $\text{H}^{\text{Pz}4}$), 5.15 (dd, 1H, $\text{H}^{\text{Thp}2}$, $^3J = 1.7$ Hz, $^3J = 10.1$ Hz), 3.49 (m, 1H, $\text{H}^{\text{Thp}6}$), 3.31 (s, 3H, NCH_3), 3.29 (s, 3H, NCH_3), 3.25 (s, 3H, NCH_3), 3.19 (s, 3H, NCH_3), 2.92 (m, 1H, $\text{H}^{\text{Thp}6}$), 1.92–2.10 (m, 25H, $\text{CCH}_3 + \text{H}^{\text{Thp}3}$), 1.70–1.80 (m, 1H, $\text{H}^{\text{Thp}4}$), 1.60–1.70 (m, 1H, $\text{H}^{\text{Thp}3}$), 1.29 (m, 3H, $\text{H}^{\text{Thp}4} + 5$) ppm. ^{13}C NMR (DMSO): δ 152.1 ($\text{C}^{\text{Pz}3}$), 145.7 ($\text{C}^{\text{Im}2}$), 145.4 ($\text{C}^{\text{Im}2}$), 144.8 ($\text{C}^{\text{Im}2}$), 144.7 ($\text{C}^{\text{Im}2}$), 143.5 ($\text{C}^{\text{Pz}5}$), 129.8 ($\text{C}^{\text{Im}5}$), 129.1 ($\text{C}^{\text{Im}5}$), 128.9 ($\text{C}^{\text{Im}5}$), 128.8 ($\text{C}^{\text{Im}5}$), 124.6 ($\text{C}^{\text{Im}4}$), 124.5 ($\text{C}^{\text{Im}4}$), 124.4 ($\text{C}^{\text{Im}4}$), 124.3 ($\text{C}^{\text{Im}4}$), 105.6 ($\text{C}^{\text{Pz}4}$), 84.4 ($\text{C}^{\text{Thp}2}$), 71.2 (COCH_3), 70.9 (COCH_3), 66.7 ($\text{C}^{\text{Thp}6}$), 31.7 (NCH_3), 31.4 (NCH_3), 31.2 (NCH_3), 31.0 (NCH_3), 29.1 ($\text{C}^{\text{Thp}3}$), 24.5 ($\text{C}^{\text{Thp}5}$), 22.6 ($\text{C}^{\text{Thp}4}$), 12.4 (CCH_3), 12.4 (CCH_3), 12.3 (CCH_3), 12.3 (CCH_3), 8.5 (CCH_3), 8.4 (CCH_3), 8.4 (CCH_3), 8.3 (CCH_3) ppm. IR (KBr): 3398 (br), 2942 (s), 2921 (s), 2861 (s), 2737 (m), 1728 (s), 1636 (m), 1602 (s), 1444 (vs), 1402 (s), 1371 (s), 1301 (m), 1252 (m), 1220 (m), 1205 (m), 1181 (m), 1135 (m), 1083 (s), 1061 (s), 1043 (s), 1008 (m), 929 (w), 907 (m), 876 (m), 823 (w), 770 (m), 730 (s), 688 (w), 562 (w), 459 (w). mp: 150 °C (decomp.). Anal. Calcd for $\text{C}_{34}\text{H}_{48}\text{N}_{10}\text{O}_3 \cdot 0.6\text{CH}_2\text{Cl}_2$ (695.78): C, 59.73; H, 7.13; N, 20.13. Found: C, 59.87; H, 7.38; N, 19.94.

3,5-Bis-[bis-(1,4,5-trimethylimidazol-2-yl)-methoxymethyl]-1-tetrahydropyran-2-yl-pyrazole (3b**)**. To a suspension of sodium hydride (1.70 g, 70.6 mmol) in dry THF (250 mL) a solution of **2b** (18.50 g, 28.2 mmol) in dry THF (90 mL) was added dropwise under N_2 . The red suspension was stirred for 2 h, and methyl iodide (4.9 mL, 70.6 mmol) was then added. After stirring overnight, the reaction mixture was quenched by adding half-saturated sodium chloride solution (60 mL). The organic solvent was removed under reduced pressure, and the aqueous phase extracted with chloroform (7 × 60 mL). The organic layer was dried over MgSO_4 , filtered, and the solvent removed under reduced pressure to give **3b** as a yellowish solid (18.98 g, 28.2 mmol, 100%).

MS (FAB⁺) m/z (relative intensity): 673.4 (100, $[\text{M} + \text{H}]^+$), 525.3 (22, $[\text{M} - 2\text{OCH}_3 - \text{thp}]^+$), 433.2 (18, $[\text{M} - 2\text{Tri} - \text{thp}]^+$), 247 (10, $[\text{C}(\text{OH})(\text{Tri})_2]^+$), 111 (56, $[\text{Tri} + \text{H}]^+$). ^1H NMR (CDCl_3): δ 6.39 (s, 1H, $\text{H}^{\text{Pz}4}$), 5.55 (dd, 1H, $\text{H}^{\text{Thp}2}$, $^3J = 1.4$ Hz, $^3J = 4.3$ Hz), 3.58–3.71 (m, 1H, $\text{H}^{\text{Thp}3}$), 3.30 (s, 3H, NCH_3), 3.28 (s, 3H, OCH_3), 3.26 (s, 3H, OCH_3), 3.23 (d, 1H, $\text{H}^{\text{Thp}3}$), 3.21 (s, 3H, NCH_3), 3.18 (s, 3H, NCH_3), 3.11 (s, 3H, NCH_3), 1.88–2.20 (m, 26H, CCH_3 and $\text{H}^{\text{Thp}6}$), 1.62–1.84 (m, 1H, $\text{H}^{\text{Thp}5}$), 1.21–1.57 (m, 3H, $\text{H}^{\text{Thp}4} + 5$) ppm. ^{13}C NMR (CDCl_3): δ 150.4 ($\text{C}^{\text{Pz}5}$), 143.1 ($\text{C}^{\text{Im}2}$), 143.0 ($\text{C}^{\text{Im}2}$), 141.8 ($\text{C}^{\text{Im}2}$), 141.6 ($\text{C}^{\text{Im}2}$), 140.0 ($\text{C}^{\text{Pz}3}$), 131.0 ($\text{C}^{\text{Im}4}$), 130.9

(C^{Im4}), 130.7 (C^{Im4}), 130.6 (C^{Im4}), 124.8 (C^{Im5}), 124.7 (C^{Im5}), 124.3 (C^{Im5}), 124.2 (C^{Im5}), 108.7 (C^{Pz4}), 85.0 (C^{Thp2}), 78.2 (COCH₃), 77.2 (COCH₃), 67.5 (C^{Thp6}), 53.7 (OCH₃), 53.2 (OCH₃), 32.0 (NCH₃), 31.9 (NCH₃), 31.6 (NCH₃), 31.5 (NCH₃), 29.5 (C^{Thp3}), 24.8 (C^{Thp5}), 22.7 (C^{Thp4}), 12.9 (CCH₃), 12.8 (CCH₃), 12.7 (CCH₃), 12.6 (CCH₃), 8.9 (CCH₃), 8.9 (CCH₃), 8.8 (CCH₃), 8.8 (CCH₃) ppm. IR (KBr): 3423 (br), 2942 (s), 2939 (vs), 2860 (s), 1693 (m), 1647 (m), 1600 (s), 1442 (vs), 1398 (vs), 1354 (m), 1300 (m), 1251 (m), 1205 (m), 1135 (m), 1082 (s), 1038 (s), 1010 (m), 947 (m), 906 (m), 874 (m), 820 (m), 763 (m), 729 (s), 698 (m), 558 (w). mp: 133 °C (decomp.). Anal. Calcd for C₃₆H₅₂N₁₀O₃·0.6CHCl₃ (744.51): C, 59.05; H, 7.12; N, 18.81. Found: C, 59.41; H, 7.47; N, 18.56.

3,5-Bis-[bis-(1,4,5-trimethylimidazol-2-yl)-methoxymethyl]-pyrazole hydrochloride (HL²·HCl). A solution of **3b** (11.13 g, 16.6 mmol) in ethanolic HCl (80 mL) was stirred overnight. The solvent was evaporated under reduced pressure, and the crude product redissolved in CHCl₃ (50 mL). The resulting solution was slowly dropped into Et₂O (600 mL). The resulting light yellow precipitate was collected by filtration and dried in vacuum to give HL²·HCl (10.00 g, 16.0 mmol, 97%) as a yellowish solid.

MS (FAB⁺) *m/z* (relative intensity): 589 (100, [M - Cl]⁺). ¹H NMR (DMSO): δ 7.34 (s, 1H, H^{Pz4}), 3.56 (s, 12H, NCH₃), 3.33 (s, 6H, OCH₃), 2.31 (s, 12H, CCH₃), 2.23 (s, 12H, CCH₃) ppm. ¹³C NMR (DMSO): δ 140.2 (C^{Pz3+5}), 135.9 (C^{Im2}), 130.7 (C^{Im4}), 126.1 (C^{Im5}), 109.7 (C^{Pz4}), 74.1 (COCH₃), 54.0 (OCH₃), 33.2 (NCH₃), 9.1 (CCH₃), 8.4 (CCH₃) ppm. IR (KBr, cm⁻¹): 3485 (br), 3059 (m), 2943 (m), 2877 (m), 2751 (m), 1648 (vs), 1520 (s), 1445 (s), 1381 (w), 1323 (m), 1262 (m), 1225 (m), 1201 (w), 1170 (w), 1083 (s), 1033 (m), 996 (w), 959 (w), 895 (m), 751 (m), 563 (m). mp: 192 °C (decomp.).

3,5-Bis-[bis-(1,4,5-trimethylimidazol-2-yl)-methoxymethyl]-pyrazole (HL²). A suspension of the hydrochloride HL²·HCl (10.00 g, 16.0 mmol) in ammoniacal CH₂Cl₂ (100 mL) was stirred overnight. The solution was then filtered, dried over MgSO₄, and the solvent removed under reduced pressure to yield HL² as a brownish solid (6.96 g, 11.8 mmol, 74%).

MS (EI) *m/z* (relative intensity): 588 (5, [M]⁺), 573 (10, [M - CH₃]⁺), 558 (2, [M - 2CH₃]⁺), 541 (12, [M - CH₃ - OCH₃]⁺), 525 (2, [M - 2OCH₃]⁺), 313 (24, [M - CH₃ - C(Im)₂OCH₃]⁺), 110 (100, [Tri]⁺). ¹H NMR (CDCl₃): δ 6.21 (s, 1H, H^{Pz4}), 3.31 (s, 12H, NCH₃), 3.03 (s, 6H, OCH₃), 2.01 (s, 12H, CCH₃), 1.95 (s, 12H, CCH₃) ppm. ¹³C NMR (CDCl₃): δ 146.50 (C^{Pz3+5}), 142.30 (C^{Im2}), 130.53 (C^{Im4}), 124.71 (C^{Im5}), 106.23 (C^{Pz4}), 75.80 (COCH₃), 52.12 (OCH₃), 31.03 (NCH₃), 12.31 (CCH₃), 8.66 (CCH₃) ppm. IR (KBr, cm⁻¹): 3255 (br), 2921 (s), 2862 (m), 2825 (m), 1722 (m), 1635 (m), 1601 (s), 1542 (m), 1476 (s), 1443 (s), 1398 (s), 1301 (m), 1262 (s), 1231 (m), 1131 (m), 1075 (vs), 1013 (s), 949 (m), 899 (s), 802 (s), 747 (vs), 659 (m). mp: 132 °C (decomp.).

3,5-Bis-[bis-(1,4,5-trimethylimidazol-2-yl)-hydroxymethyl]-pyrazole hydrochloride (H₃L⁵·HCl). A solution of **2b** (18.55 g, 28.8 mmol) in ethanolic HCl (50 mL) was stirred overnight. The solvent was then evaporated and the crude product redissolved in CHCl₃ (100 mL). The resulting solution was slowly dropped into Et₂O (700 mL). A white flocculent precipitate formed that was collected by filtration and dried in vacuum to give H₃L⁵·HCl (16.83 g, 28.2 mmol, 98%) as a light gray solid.

MS (FAB⁺) *m/z* (relative intensity): 561 (100, [M]⁺), 451 (6, [M - Tri]⁺), 341 (68, [M - 2Tri]⁺), 110 (77, [Tri]⁺). ¹H NMR (DMSO): δ 12.50–15.50 (br, 2H, NH), 9.56 (br, 2H, OH), 7.05 (s, 1H, H^{Pz4}), 3.56 (s, 12H, NCH₃), 2.26 (s, 12H, CCH₃), 2.21 (s, 12H, CCH₃) ppm. ¹³C NMR (DMSO): δ 138.5 (C^{Im2}), 133.1 (C^{Im4}), 125.3 (C^{Im5}), 107.5 (C^{Pz4}), 68.2 (COH), 33.2 (NCH₃), 8.9 (CCH₃), 8.3 (CCH₃) ppm. IR (KBr, cm⁻¹): 3408 (br), 3051 (vs), 2960 (vs),

2886 (s), 2752 (s), 2084 (br), 1649 (vs), 1520 (s), 1444 (s), 1385 (m), 1323 (m), 1264 (m), 1224 (m), 1192 (m), 1074 (m), 1018 (w), 996 (w), 898 (m), 830 (m), 749 (m), 566 (w). mp: 198 °C (decomp.).

3,5-Bis-[bis-(1,4,5-trimethylimidazol-2-yl)-hydroxymethyl]-pyrazole (H₃L⁵). The hydrochloride H₃L⁵·HCl (16.83 g, 28.2 mmol) was dissolved in ammoniacal CH₂Cl₂ (150 mL), and the solution stirred overnight. The solvent was then removed under reduced pressure, and the crude product redissolved in CH₂Cl₂ (50 mL). This solution was slowly dropped into *n*-hexane (400 mL), and the resulting white precipitate was separated by filtration and dried in vacuum to yield H₃L⁵ as a light gray solid (9.00 g, 16.1 mmol, 57%).

MS (EI) *m/z* (relative intensity): 560 (5, [M]⁺), 450 (36, [M - Tri]⁺), 340 (36, [M - 2Tri]⁺), 110 (100, [Tri]⁺). ¹H NMR (DMSO): δ 5.92 (s, 1H, H^{Pz4}), 3.18 (s, 12H, NCH₃), 1.99 (s, 24H, CCH₃) ppm. ¹³C NMR (DMSO): δ 148.7 (C^{Pz3+5}), 129.4 (C^{Im4}), 125.5 (C^{Im5}), 104.7 (C^{Pz4}), 69.9 (COH), 31.5 (NCH₃), 11.7 (CCH₃), 8.6 (CCH₃) ppm. IR (KBr, cm⁻¹): 3452 (br), 3098 (br), 2954 (m), 2923 (m), 2860 (m), 2761 (m), 1717 (s), 1671 (s), 1603 (m), 1445 (m), 1404 (m), 1301 (m), 1223 (w), 1138 (w), 1056 (m), 997 (m), 905 (s), 806 (m), 765 (w), 731 (w), 653 (w), 567 (w). mp: 198 °C (decomp.).

3,5-Bis-[bis-(4,5-diphenyl-1-methylimidazol-2-yl)-hydroxymethyl]-1-tetrahydropyran-2-yl-pyrazole (2c). To a suspension of 4,5-diphenyl-1-methylimidazole (44.30 g, 189.0 mmol) in dry THF (1000 mL) *n*-Butyllithium (130 mL, 208 mmol, 1.6 M in *n*-hexane) was added dropwise under N₂. The dark brown solution was stirred for 1.5 h at room temperature. A solution of **1** (12.68 g, 47.3 mmol) in dry THF (300 mL) was added, and the resulting reaction mixture stirred overnight. The reaction mixture was then quenched by the addition of half-saturated ammonium chloride solution (50 mL). All volatiles were removed under reduced pressure, and the crude product redissolved in ammoniacal CH₂Cl₂ (400 mL). The solution was filtered and dried over MgSO₄. After evaporation of the solvent **2c** was obtained as a white solid (48.90 g, 42.8 mmol, 91%).

MS (FAB⁺) *m/z* (relative intensity) 1141.7 (30, [M + H]⁺), 1057.5 (3, [M + H - thp]⁺), 589.3 (100, [M + H - thp - 2Di]⁺), 235.2 (66, [Di + H]⁺). ¹H NMR (CDCl₃): δ 7.05–7.50 (m, 10 H, H^{Ph}), 6.34 (s, 1 H, OH), 6.81 (s, 1 H, OH), 6.16 (s, 1 H, H^{Pz4}), 5.56 (dd, 1 H, ³J = 1.9 Hz, ³J = 10 Hz, H^{Thp2}), 3.75 (m, 1 H, H^{Thp6}), 3.57 (s, 3 H, NCH₃), 3.39 (s, 3 H, NCH₃), 3.35 (s, 3 H, NCH₃), 3.30 (s, 3 H, NCH₃), 3.17 (m, 1 H, H^{Thp6}), 2.34 (m, 1 H, H^{Thp3}), 1.87 (m, 3 H, 2 H^{Thp3+4}), 1.35 (m, 2 H, H^{Thp5}) ppm. ¹³C NMR (CDCl₃): δ 152.6 (C^{Pz5}), 146.8 (C^{Im2}), 146.8 (C^{Im2}), 146.7 (C^{Im2}), 145.9 (C^{Im2}), 142.0 (C^{Pz3}), 135.7 (C^q), 135.1 (C^q), 134.0 (C^q), 133.7 (C^q), 134.6 (C^q), 134.4 (C^q), 131.9 (C^q), 131.4 (C^q), 131.4 (C^q), 131.3 (C^q), 130.8 (C^q), 131.1 (C^{Ph}), 131.0 (C^{Ph}), 131.0 (C^{Ph}), 129.0 (C^{Ph}), 128.9 (C^{Ph}), 128.9 (C^{Ph}), 128.6 (C^{Ph}), 128.6 (C^{Ph}), 128.0 (C^{Ph}), 127.9 (C^{Ph}), 127.9 (C^{Ph}), 126.6 (C^{Ph}), 126.5 (C^{Ph}), 126.1 (C^{Ph}), 126.0 (C^{Ph}), 126.0 (C^{Ph}), 108.7 (C^{Pz4}), 85.0 (C^{Thp2}), 71.7 (COH), 70.3 (COH), 68.0 (C^{Thp6}), 33.2 (NCH₃), 32.7 (NCH₃), 32.6 (NCH₃), 32.5 (NCH₃), 29.3 (C^{Thp5}), 24.8 (C^{Thp3}), 22.8 (C^{Thp4}) ppm. IR (KBr, cm⁻¹): 3367 (br), 3056 (s), 2947 (s), 2858 (m), 1954 (w), 1889 (w), 1810 (w), 1772 (w), 1602 (vs), 1505 (vs), 1472 (m), 1443 (s), 1387 (m), 1353 (m), 1319 (m), 1250 (m), 1234 (m), 1205 (m), 1178 (m), 1139 (s), 1071 (m), 1059 (s), 1041 (s), 1025 (s), 1006 (m), 970 (s),

907 (s), 874 (m), 820 (w), 773 (vs), 720 (m), 694 (vs), 647 (m). mp: 179 °C. Anal. Calcd for $C_{74}H_{64}N_{10}O_3 \cdot (0.4CH_2Cl_2)$ (1175.37): C, 76.03; H, 5.56; N, 11.92. Found: C, 76.22; H, 5.80; N, 11.81.

3,5-Bis-[bis-(4,5-diphenyl-1-methylimidazol-2-yl)-methoxymethyl]-1-tetrahydropyran-2-ylpyrazole (3c). To a solution of **2c** (10.00 g, 8.8 mmol) in dry THF (150 mL) under N_2 was added sodium hydride (0.53 g, 22.0 mmol). The suspension was stirred for 2 h, and methyl iodide (1.37 mL, 3.11 g, 22.0 mmol) was then added. After the reaction mixture was stirred overnight, it was quenched by adding half-saturated sodium chloride solution (60 mL). THF was removed under reduced pressure, and the aqueous phase was extracted with $CHCl_3$ (3 \times 50 mL). The combined organic phases were dried over $MgSO_4$. After evaporating the solvent **3c** was obtained as a yellow solid (9.42 g, 8.1 mmol, 92%).

MS (FAB⁺) *m/z* (relative intensity): 1191.7 (92, [M + Na]⁺), 1169.8 (100, [M + H]⁺), 1085.6 (27, [M - thp + H]⁺), 993.5 (31, [M - thp - Ph - O]⁺), 805.3 (38, [M - thp - Di - OCH₃ - OH]⁺), 247.0 (82, [Di + CH₂]⁺). ¹H NMR (CDCl₃): δ 7.05–7.50 (m, 10 H, H^{Ph}), 6.85 (s, 1 H, H^{Pz4}), 5.75 (m, 1 H, H^{Thp2}), 3.72 (m, 1 H, H^{Thp6}), 3.79 (s, 3 H, NCH₃), 3.66 (s, 3 H, NCH₃), 3.62 (s, 6 H, OCH₃, NCH₃), 3.47 (s, 6 H, OCH₃, NCH₃), 3.17 (m, 1 H, H^{Thp6}), 2.45 (m, 1 H, H^{Thp3}), 1.87 (m, 3 H, H^{Thp3 + 4}), 1.30 (m, 2 H, H^{Thp5}) ppm. ¹³C NMR (CDCl₃): 149.4 (C^{Pz5}), 145.6 (C^{Im2}), 145.3 (C^{Im2}), 144.0 (C^{Im2}), 143.5 (C^{Im2}), 140.7 (C^{Pz3}), 135.7, 135.6, 135.5, 135.1, 135.0, 135.0, 134.8, 131.5, 131.5, 131.2, 131.0, 130.9, 130.9, 128.9, 128.8, 128.5, 128.4, 128.0, 127.9, 127.8, 127.7, 126.5, 126.4, 125.9, 125.8, 125.7, 110.0 (C^{Pz4}), 85.3 (C^{Thp2}), 79.1 (COCH₃), 78.1 (COCH₃), 68.0 (C^{Thp6}), 54.5 (OCH₃), 54.2 (OCH₃), 33.0 (NCH₃), 32.9 (NCH₃), 32.8 (NCH₃), 32.6 (NCH₃), 29.7 (C^{Thp3}), 24.9 (C^{Thp5}), 22.8 (C^{Thp4}) ppm. IR (KBr, cm⁻¹): 3444 (br), 3055 (m), 3029 (m), 2939 (m), 2856 (m), 2831 (m), 1956 (w), 1891 (w), 1820 (w), 1756 (w), 1689 (w), 1603 (s), 1576 (m), 1505 (s), 1443 (s), 1384 (m), 1353 (w), 1319 (m), 1236 (m), 1205 (m), 1179 (m), 1131 (m), 1072 (s), 1025 (s), 968 (m), 907 (m), 890 (m), 874 (m), 844 (w), 819 (w), 773 (vs), 722 (m), 695 (s), 647 (w), 613 (w), 523 (m). mp: 230 °C (decomp.). Anal. Calcd for $C_{76}H_{68}N_{10}O_3 \cdot (0.1CH_2Cl_2)$ (1177.94): C, 77.60; H, 5.84; N, 11.89. Found: C, 77.59; H, 6.15; N, 11.85.

3,5-Bis-[bis-(4,5-diphenyl-1-methylimidazol-2-yl)-methoxymethyl]pyrazole hydrochloride (HL³·HCl). A solution of **3c** (9.42 g, 8.1 mmol) in ethanolic hydrochloride (50 mL) was stirred overnight at room temperature. The solvent was then removed under reduced pressure, and the crude product redissolved in $CHCl_3$ (50 mL). This solution was slowly dropped into Et₂O (600 mL) to give a white precipitate that was separated by filtration. After drying in vacuum, **HL³·HCl** was obtained as a white solid (8.94 g, 8.0 mmol, 99%).

MS (FAB⁺) *m/z* (relative intensity): 1085.5 (100, [M - Cl]⁺), 805.2 (9, [M - Cl - Di - 3CH₃]⁺), 543.1 (16, [M - Cl + H]²⁺), 235.0 (24, [Di + H]⁺) ¹H NMR (DMSO): δ 7.34–7.57 (m, 40 H, H^{Ph}), 7.20 (s, 1 H, H^{Pz4}), 3.49 (s, 6 H, OCH₃), 3.38 (s, 12 H, NCH₃) ppm. ¹³C NMR (DMSO): δ 144.3 (C^{Pz3 + 5}), 142.1 (C^{Im2}), 132.5 (C^{i-Ph}), 132.4 (C^{i-Ph}), 131.1 (C^{o/m-Ph}), 130.3 (C^{Im4}), 129.8 (C^{P-Ph}), 129.2 (C^{o/m-Ph}), 128.3 (C^{o/m-Ph}), 127.9 (C^{P-Ph}), 127.7 (C^{Im5}), 127.4 (C^{o/m-Ph}), 110.3 (C^{Pz4}), 79.4 (COCH₃), 53.4 (OCH₃), 33.3 (NCH₃) ppm. IR (KBr, cm⁻¹): 3402 (br), 3040 (s), 2963 (s), 1632 (m), 1596 (m), 1503 (m), 1477 (m), 1445 (s), 1418 (m), 1323 (m), 1289 (m), 1233 (w), 1183 (w), 1075 (s), 1025 (s), 978 (m), 902 (m), 770 (s), 696 (vs). mp: 145 °C (decomp.). Anal. Calcd for $C_{71}H_{61}ClN_{10}O_2 \cdot (4.9HCl + 0.4EtOH)$ (1318.88): C, 65.39; H, 5.22; N, 10.62; Cl, 15.86. Found: C, 64.98; H, 5.67; N, 10.95; Cl, 15.70.

3,5-Bis-[bis-(4,5-Diphenyl-1-methylimidazol-2-yl)-methoxymethyl]pyrazole (HL³). The hydrochloride **HL³·HCl** (57.73 g, 52.7 mmol) was dissolved in ammoniacal CH_2Cl_2 (600 mL) and stirred

for 4 h at room temperature. After filtration all volatiles were evaporated under reduced pressure. The crude product was redissolved in CH_2Cl_2 (50 mL) and slowly dropped into *n*-hexane (300 mL). A white precipitate formed that was collected by filtration and redissolved in CH_2Cl_2 . Finally the solvent was removed, and the remaining solid dried in vacuum to give **HL³** as a white solid (31.95 g, 30.2 mmol, 58%).

MS (FAB⁺) *m/z* (relative intensity): 1085.5 (100, [M + H]⁺), 1069.4 (35, [M + H - CH₃]⁺), 993.4 (28, [M + H - Ph - CH₃]⁺), 805.3 (28, [M + H - Di - 3CH₃]⁺), 504.2 (16, [M + 2H]²⁺), 247.1 (80, [Di + CH₂]⁺), 118.1 (80, [Di + H]⁺). ¹H NMR (CDCl₃): δ 13.70 (s, 1 H, NH), 7.05–7.50 (m, 40 H, H^{Ph}), 6.87 (s, 1 H, H^{Pz4}), 3.55 (s, 6 H, OCH₃), 3.41 (s, 12 H, NCH₃) ppm. ¹³C NMR (CDCl₃): δ 144.9 (C^{Pz3 + 5}), 135.8 (C^q), 134.6 (C^q), 131.1 (C^q), 131.0 (C^{o/m-Ph}), 128.9 (C^{o/m-Ph}), 128.5 (C^{P-Ph}), 127.9 (C^{o/m-Ph}), 126.8 (C^{o/m-Ph}), 126.0 (C^{P-Ph}), 108.3 (C^{Pz4}), 76.4 (COCH₃), 53.4 (OCH₃), 33.5 (NCH₃) ppm. IR (KBr, cm⁻¹): 3244 (br), 3055 (m), 2948 (m), 2826 (m), 1951 (w), 1886 (w), 1809 (w), 1602 (s), 1504 (s), 1442 (s), 1384 (m), 1318 (w), 1266 (w), 1234 (w), 1126 (w), 1072 (s), 1024 (m), 968 (m), 902 (m), 816 (w), 773 (vs), 745 (m), 720 (m), 694 (vs), 522 (m). mp: 161 °C (decomp.). Anal. Calcd for $C_{71}H_{60}N_{10}O_2 \cdot (0.2CH_2Cl_2)$ (1102.32): C, 77.58; H, 5.52; N, 12.71. Found: C, 77.57; H, 5.43; N, 12.69.

3,5-Bis-[bis-(4,5-diphenyl-1-methylimidazol-2-yl)-hydroxymethyl]-pyrazole hydrochloride (H₃L⁶·HCl). A solution of **2c** (11.32 g, 9.9 mmol) in ethanolic hydrochloride (50 mL) was stirred at room temperature for 5 h. The solvent was then evaporated under reduced pressure, and the crude product redissolved in methanol (20 mL). This solution was slowly dropped into Et₂O (400 mL) and the resulting white precipitate collected by filtration. After drying in vacuum, **H₃L⁶·HCl** was obtained as a light gray solid (7.77 g, 7.1 mmol, 72%).

MS (FAB⁺) *m/z* (relative intensity): 1057.5 (73, [M + H]⁺), 823.3 (13, [M + H - Di]⁺), 589.3 (97, [M + H - 2Di]⁺), 235.2 (100, [Di + H]⁺). ¹H NMR (DMSO): δ 7.21–7.54 (m, 40 H, H^{Ph}), 7.05 (s, 1 H, H^{Pz4}), 3.48 (s, 12 H, NCH₃) ppm. ¹³C NMR (DMSO): δ 146.1 (C^{Pz3 + 5}), 144.5 (C^{Im2}), 132.0 (C^q), 131.6 (C^q), 130.9 (C^{o/m-Ph}), 129.8 (C^{P-Ph}), 129.7 (C^q), 129.2 (C^{o/m-Ph}), 128.2 (C^{o/m-Ph}), 127.9 (C^{P-Ph}), 127.5 (C^q), 127.4 (C^{o/m-Ph}), 106.9 (C^{Pz4}), 71.3 (COH), 33.8 (NCH₃) ppm. IR (KBr, cm⁻¹): 3407 (br), 3054 (m), 2961 (m), 2726 (m), 1955 (w), 1827 (br), 1632 (w), 1596 (w), 1504 (m), 1478 (m), 1445 (s), 1420 (w), 1324 (w), 1286 (w), 1232 (w), 1184 (w), 1126 (w), 1074 (m), 1025 (m), 972 (w), 902 (m), 770 (s), 697 (vs), 611 (w), 520 (m). mp: 166 °C (decomp.). Anal. Calcd for $C_{69}H_{57}N_{10}O_2Cl \cdot (3HCl)$ (1203.12): C, 68.88; H, 5.03; N, 11.64. Found: C, 68.78; H, 5.13; N, 11.64.

3,5-Bis-[bis-(4,5-diphenyl-1-methylimidazol-2-yl)-hydroxymethyl]-pyrazole (H₃L⁶). The hydrochloride **H₃L⁶·HCl** (7.77 g, 7.1 mmol) was dissolved in ammoniacal CH_2Cl_2 (150 mL), and the solution stirred at room temperature overnight. The reaction mixture was then filtered and dried over $MgSO_4$. After evaporation of the solvent and drying of the product in vacuum, **H₃L⁶** was obtained as a yellowish solid (4.66 g, 4.4 mmol, 62%).

MS (FAB⁺) *m/z* (relative intensity): 1057.4 (93, [M + H]⁺), 823.3 (14, [M - Di]⁺), 589.2 (100, [M - 2Di]⁺), 235.2 (76, [Di + H]⁺) ¹H NMR (CDCl₃): δ 7.10–7.45 (m, 40 H, H^{Ph}) 6.41 (s, 1 H, H^{Pz4}), 3.31 (s, 12 H, NCH₃) ppm. ¹³C NMR (CDCl₃): δ 146.3 (C^{Im2}), 135.2 (C^q), 134.2 (C^q), 131.5 (C^q), 130.9 (C^{o/m-Ph}), 130.5 (C^q), 128.9 (C^{o/m-Ph}), 128.7 (C^{P-Ph}), 127.9 (C^{o/m-Ph}), 126.5 (C^{o/m-Ph}), 126.2 (C^{P-Ph}), 104.7 (C^{Pz4}), 70.1 (COH), 32.2 (NCH₃) ppm. IR (KBr, cm⁻¹): 3339 (br), 3167 (m), 3052 (m), 2951 (m), 1955 (w), 1889 (w), 1810 (w), 1638 (w), 1602 (s), 1559 (w), 1504 (s), 1442 (s), 1383 (m), 1319 (w), 1265 (w), 1230 (w), 1130 (m), 1058 (s), 1025

(s), 966 (s), 899 (s), 772 (vs), 730 (m), 694 (vs), 522 (w). mp: 197 °C. Anal. Calcd for $C_{69}H_{56}N_{10}O_2 \cdot (0.2CH_2Cl_2)$ (1073.25): C, 77.44; H, 5.20; N, 13.05. Found: C, 77.23; H, 5.22; N, 13.06.

[$L^2Ni(NO_3)_2(MeOH)_2Ni$] (4). HL^2 (300 mg, 0.51 mmol) was dissolved in MeOH (50 mL) and 2 equiv of KO^tBu (57 mg, 0.51 mmol) were added. After stirring for 15 min, 2 equiv of $Ni(NO_3)_2 \cdot 6H_2O$ (223 mg, 0.76 mmol) were added, and the resulting solution stirred for further 5 h at room temperature. The solvent was then removed under reduced pressure, and the residue redissolved in MeOH (20 mL). After filtration, the solution was layered in a Schlenk tube first with a MeOH/Et₂O mixture (1:1, 20 mL) and then with pure Et₂O (80 mL). Green crystals of **4** (140.5 mg, 0.09 mmol, 33%) gradually formed that were suitable for X-ray analysis.

IR (KBr, cm^{-1}) 3564 (s), 3418 (br), 2934 (s), 2827 (w), 2604 (w), 1892 (br), 1619 (s), 1488 (vs), 1445 (s), 1408 (s), 1384 (s), 1352 (s), 1295 (vs), 1220 (m), 1119 (m), 1085 (m), 1027 (m), 995 (m), 916 (s), 826 (m), 811 (m), 784 (m), 739 (w), 522 (w). UV-vis (DMF) λ [nm] (ϵ [$M^{-1}cm^{-1}$]) 646 (32). UV-vis (KBr, diffuse reflectance) λ [nm] 644, 345, 245. MS (ESI, MeOH) m/z (%) 1534.5 (25, [$L^2Ni_3(NO_3)_3$]³⁺), 736.4 (47, [$L^2Ni_3(NO_3)_2$]²⁺), 645.4 (100, [L^2Ni]⁺). HR-MS (ESI, MeOH): calcd for $C_{62}H_{86}N_{22}O_{10}Ni_3$ ([$L^2Ni_3(NO_3)_2$]²⁺) 736.2473, found 736.2469.

[$L^2NiCl(MeOH)_2Ni$]Cl₂ (5). To a solution of HL^2 (500 mg, 0.85 mmol) in MeOH were added 2 equiv of KO^tBu (95 mg, 0.85 mmol). After stirring for 15 min, 2 equiv of $NiCl_2 \cdot 6H_2O$ (303 mg, 1.27 mmol) were added, and the solution was stirred for further 5 h. The solvents were removed in vacuo, and the residue was redissolved in 20 mL methanol. After filtration into a Schlenk tube, the complex solution was layered first with 20 mL of methanol: diethylether (1:1) and then with 80 mL diethylether. The resulting yellow brown crystals of **5** (407.8 mg, 0.25 mmol, 60%) were suitable for X-ray analysis.

IR (KBr, cm^{-1}) 3393 (br), 2924 (m), 2833 (w), 2566 (w), 1651 (m), 1620 (m), (vs), 1445 (m), 1410 (m), 1340 (w), 1306 (w), 1224 (m), 1168 (w), 1114 (m), 1076 (m), 1033 (s), 1024 (s), 994 (m), 967 (w), 916 (s), 879 (s), 779 (m), 739 (w), 521 (w). UV-vis (MeCN) λ [nm] (ϵ [$M^{-1}cm^{-1}$]) 726 (44), 426 (151), 239 (52100), 203 (80840). UV-vis (KBr, diffuse reflectance) λ [nm] 706, 415, 242.

[$L^3Cu_2(PMe_3)_2(PF_6)_2$ (6). In a 50 mL Schlenk flask HL^5 (500 mg, 0.46 mmol) and KO^tBu (51 mg, 0.46 mmol) were dissolved in 10 mL of THF. A solution of $[Cu(MeCN)_4]PF_6$ (343 mg, 0.92 mmol) in 10 mL of acetonitrile was added, and the resulting solution was stirred for 15 min. Finally, trimethylphosphin (0.92 mL, 0.92 mmol, 1.0 M solution in THF) was added, and the reaction mixture stirred for additional 15 min. The solvent was removed in vacuum, the resulting solid redissolved in dichloromethane (6 mL) and filtrated. Purple crystals of **6** $\cdot CH_2Cl_2 \cdot Et_2O$ (279.8 mg, 0.1 mmol, 42%) suitable for X-ray analysis were obtained by vapor diffusion of diethyl ether in the dichloromethane solution.

MS (ESI) m/z (relative intensity): 1363.6 (13, [$L^5Cu_2(PMe_3)_2$]⁺), 1287.4 (24, [$L^5Cu_2(PMe_3)_3$]⁺), 1223.5 (6, [$L^5Cu(PMe_3)_3$]⁺), 1147.4 (100, [L^5Cu]⁺). ¹H NMR (CD₃CN): δ 6.90–7.55 (m, 32 H, H^{Ph}), 6.35–6.90 (m, 8 H, H^{Ph}), 3.25–3.70 (m, 18 H, NCH₃ + OCH₃), 0.21 (d, 6 H, ²J = 7.0 Hz, PCH₃) ppm. ¹³C NMR (CD₃CN): δ 149.3, 148.0, 146.8, 145.4, 137.1, 135.0, 132.5, 132.2, 132.1, 131.0, 130.3, 130.2, 130.0, 130.0, 129.7, 129.3, 129.2, 129.0, 128.9, 128.4, 128.2, 128.1, 127.7, 105.0 (C^{Pz4}), 79.7 (COCH₃), 54.0 (OCH₃), 53.6 (OCH₃), 35.4 (NCH₃), 33.7 (NCH₃), 14.9 (d, ¹J = 25.8 Hz, C^{PMe3}) ppm. ³¹P NMR (CD₃CN): δ -44.8 (br, P^{PMe3}), -46.7 (s, P^{PMe3}), -144.2 (sept, P^{PF6}) ppm. IR (KBr, cm^{-1}) 3352 (br), 3057 (m), 2965 (m), 2904 (m), 2833 (w), 1963 (w), 1896 (w), 1825 (w), 1603 (vs),

1577 (m), 1504 (s), 1480 (s), 1444 (vs), 1385 (s), 1307 (m), 1289 (m), 1231 (w), 1201 (w), 1141 (w), 1127 (w), 1074 (vs), 1057 (s), 1026 (s), 1000 (m), 986 (s), 961 (vs), 917 (vs), 837 (vs), 788 (s), 773 (s), 729 (m), 697 (s), 651 (w), 557 (vs), 522 (w). HR-MS (ESI, MeCN) calcd for [$L^3Cu_2(PMe_3)_2$]⁺ 1361.42927, found 1361.43109; calcd for [$L^3Cu_2(PMe_3)_3$]⁺ 1285.38509, found 1285.38571; calcd for [$L^3Cu(PMe_3)_3$]⁺ 1223.46598, found 1223.46285; calcd for [H_2L^3]⁺ 1085.49785, found 1085.49329. Anal. Calcd for $C_{148}H_{138}Cu_4F_{12}N_{20}O_4P_4 \cdot (5.6CH_2Cl_2)$ (3342.55): C, 55.19; H, 4.50; N, 8.38. Found: C, 55.14; H, 4.51; N, 8.25.

[$L^5Cu_2(nBuNC)_2(PF_6)_2$ (7). In a 50 mL Schlenk flask HL^5 (500 mg, 0.46 mmol) and KO^tBu (51 mg, 0.46 mmol) were dissolved in 10 mL of THF. A solution of $[Cu(MeCN)_4]PF_6$ (343 mg, 0.92 mmol) in 10 mL of acetonitrile was added, and the resulting solution was stirred for 15 min. After that *n*-Butylisocyanide (96 μ L, 0.92 mmol) was added, and the reaction mixture was stirred for additional 20 min. The solvent was removed in vacuum, the resulting solid redissolved in dichloromethane (6 mL) and filtrated. Light yellowish crystals of **7** $\cdot CH_2Cl_2 \cdot Et_2O$ (658.1 mg, 0.23 mmol, 100%) suitable for X-ray analysis were obtained by vapor diffusion of diethyl ether in the dichloromethane solution.

MS (ESI) m/z (relative intensity) 1377.6 (15, [$L^3Cu_2(nBuNC)_2$]⁺), 1292.3 (45, [$L^3Cu_2(nBuNC)_3$]⁺), 1147.5 (100, [L^3Cu]⁺). ¹H NMR (CD₃CN): δ 7.10–7.50 (m, 32 H, H^{Ph}), 7.06 (s, 1 H, H^{Pz4}), 7.50–7.00 (m, 8 H, H^{Ph}), 3.05–3.60 (m, 18 H, NCH₃ + OCH₃) ppm (protons of the isonitrile could not be clearly identified because of broad signals). ¹³C NMR (CD₃CN): δ 148.6, 148.1, 146.7, 145.2, 137.3, 137.3, 134.7, 133.5, 132.8, 132.7, 132.1, 132.0, 130.8, 130.1, 130.1, 130.0, 130.0, 129.9, 129.7, 129.6, 129.5, 129.4, 129.3, 129.2, 129.0, 128.9, 128.8, 128.4, 128.3, 128.2, 128.1, 128.0, 104.4 (C^{Pz4}), 80.9 (COCH₃), 79.2 (COCH₃), 54.0 (OCH₃), 52.9 (OCH₃), 42.2 (C^{Isonitrile-4}), 34.8 (NCH₃), 34.1 (NCH₃), 31.0 (C^{Isonitrile-3}), 20.1 (C^{Isonitrile-2}), 13.4 (C^{Isonitrile-1}) ppm. IR (KBr, cm^{-1}) 3055 (m), 2965 (m), 2960 (m), 2874 (m), 2833 (m), 2196 (vs), 1961 (w), 1890 (w), 1816 (w), 1773 (w), 1603 (s), 1577 (m), 1504 (s), 1480 (s), 1443 (s), 1382 (s), 1341 (m), 1231 (w), 1202 (m), 1142 (w), 1073 (vs), 1024 (s), 985 (s), 964 (w), 921 (vs), 842 (vs), 784 (s), 774 (s), 729 (m), 695 (s), 613 (w), 557 (s). HR-MS (ESI, MeCN) calcd for [$L^3Cu_2(nBuNC)_2$]⁺ 1375.48790, found 1375.49076; calcd for [$H^3L^3Cu_2(nBuNC)_2$]²⁺ 688.24759, found 688.24901. Anal. Calcd for $C_{156}H_{138}Cu_4F_{12}N_{22}O_4P_2 \cdot (3.8CH_2Cl_2)$ (3251.82): C, 58.28; H, 4.58; N, 9.60. Found: C, 58.41; H, 4.63; N, 9.58.

[$L^5Cu_2(C_6H_3(CH_3)_2NC)_2(PF_6)_2$ (8). In a 50 mL Schlenk flask HL^5 (500 mg, 0.46 mmol) and KO^tBu (51 mg, 0.46 mmol) were dissolved in 10 mL of THF. A solution of $[Cu(MeCN)_4]PF_6$ (343 mg, 0.92 mmol) in 10 mL of acetonitrile was added, and the resulting solution was stirred for 15 min. After that 2,6-dimethylphenylisocyanide (120 mg, 0.92 mmol), dissolved in acetonitrile (10 mL), was added, and the reaction mixture was stirred for additional 20 min. The solvent was removed in vacuum, the resulting solid redissolved in dichloromethane (6 mL) and filtrated. Colorless crystals of **8** $\cdot CH_2Cl_2 \cdot Et_2O$ (503.1 mg, 0.17 mmol, 74%) suitable for X-ray analysis were obtained by vapor diffusion of diethyl ether in the dichloromethane solution.

MS (ESI) m/z (relative intensity) 1473.7 (7, [$L^3Cu_2(C_6H_3(CH_3)_2NC)_2$]⁺), 1342.8 (15, [$L^3Cu_2(C_6H_3(CH_3)_2NC)_3$]⁺), 1238.5 (15, [$L^3Cu_2(CN)_2$]⁺), 1147.6 (100, [L^3Cu]⁺). ¹H NMR (CD₃CN): δ 7.10–7.50 (m, 32 H, H^{Ph}), 7.06 (s, 1 H, H^{Pz4}), 7.50–7.00 (m, 8 H, H^{Ph}), 3.05–3.60 (m, 18 H, NCH₃ + OCH₃) ppm (methyl protons of the isonitrile could not be clearly identified because of overlap with CD₃CN). ¹³C NMR (CD₃CN): δ 148.9, 147.9, 146.6, 145.4, 137.6, 137.3, 135.1, 133.8, 132.2, 132.1, 131.0, 130.3, 130.2, 130.0, 129.9, 129.8, 129.4, 128.9, 128.7, 128.5, 128.3, 128.0, 104.3 (C^{Pz4}), 79.4 (COCH₃), 79.2 (COCH₃), 54.2 (OCH₃), 51.6 (OCH₃), 34.9

Table 4. Crystal Data and Refinement Details for **2a**, **4**–**8**

	2a	4	5	6	7	8
empirical formula	C ₂₆ H ₃₂ N ₁₀ O ₃ , 2 THF, 0.25 H ₂ O	C ₆₄ H ₉₄ N ₂₄ Ni ₃ O ₁₈ , C ₄ H ₁₀ O	C ₆₆ H ₁₀₂ Cl ₂ N ₂₀ Ni ₃ O ₄ ²⁺ , 2 Cl ⁻ , 5 CH ₃ OH	C ₁₄₈ H ₁₃₆ Cu ₄ N ₂₀ O ₄ P ₂ ²⁺ , 2 PF ₆ ⁻	C ₁₅₂ H ₁₃₆ Cu ₄ N ₂₂ O ₄ ²⁺ , 2 PF ₆ ⁻ , 2 CH ₂ Cl ₂	C ₁₄₈ H ₁₃₆ Cu ₄ N ₂₀ O ₄ ²⁺ , 2 PF ₆ ⁻ , 2 C ₄ H ₁₀ O
formula weight	681.33	1737.82	1781.82	2864.91	3048.83	3123.30
crystal size [mm]	0.39 × 0.34 × 0.22	0.46 × 0.32 × 0.21	0.38 × 0.24 × 0.14	0.46 × 0.41 × 0.34	0.48 × 0.37 × 0.23	0.45 × 0.32 × 0.18
crystal system	monoclinic	triclinic	triclinic	triclinic	triclinic	triclinic
space group	<i>P</i> 2 ₁ / <i>c</i> (No. 14)	<i>P</i> $\bar{1}$ (No. 2)	<i>P</i> $\bar{1}$ (No. 2)	<i>P</i> $\bar{1}$ (No. 2)	<i>P</i> $\bar{1}$ (No. 2)	<i>P</i> $\bar{1}$ (No. 2)
<i>a</i> [Å]	11.6344(8)	10.6925(8)	10.6658(8)	14.3209(9)	14.1772(6)	14.7874(7)
<i>b</i> [Å]	15.6169(7)	14.9953(10)	15.0222(13)	15.9580(12)	16.0440(8)	17.1318(8)
<i>c</i> [Å]	19.7941(13)	15.5762(11)	15.5924(13)	20.0162(13)	20.8363(10)	18.9073(8)
α [°]	90	107.269(5)	107.507(6)	72.230(5)	68.494(4)	105.728(4)
β [°]	96.224(5)	99.014(6)	98.908(6)	85.991(5)	81.595(4)	109.984(3)
γ [°]	90	108.081(5)	108.519(6)	65.827(5)	64.366(3)	102.965(4)
<i>V</i> [Å ³]	3575.3(4)	2180.3(3)	2170.8(3)	3966.2(5)	3987.5(3)	4058.2(3)
$\rho_{\text{calcd.}}$ [g cm ⁻³]	1.266	1.324	1.363	1.199	1.270	1.278
<i>Z</i>	4	1	1	1	1	1
<i>F</i> (000)	1458	916	944	1480	1572	1620
μ [mm ⁻¹]	0.088	0.718	0.835	0.638	0.684	0.611
<i>hkl</i> range	±13, ±18, ±23	±12, ±17, ±18	-11 - 12	±16, ±18, ±23	±16, ±18, ±24	-16 - 17, ±20, ±22
θ range [°]	1.66–24.77	1.54–24.81	1.66–24.71	1.53–24.81	1.49–24.80	1.52–24.83
measured refl.	39634	22279	21500	47189	62446	61241
unique refl. [<i>R</i> _{int}]	6104 [0.0894]	7450 [0.0643]	7336 [0.0694]	13494 [0.1025]	13597 [0.0854]	13936 [0.0577]
parameters/ restraints	561/21	536/58	531/6	899/1	1000/206	974/0
goodness-of-fit	1.002	1.064	1.002	1.062	1.029	1.004
<i>R</i> 1, <i>wR</i> 2 (<i>I</i> > 2 σ (<i>I</i>))	0.0444, 0.0949	0.0689, 0.2016	0.0583, 0.1539	0.0765, 0.2096	0.0496, 0.1251	0.0341, 0.0717
<i>R</i> 1, <i>wR</i> 2 (all data)	0.0736, 0.1025	0.0851, 0.2125	0.0893, 0.1654	0.0976, 0.2226	0.0706, 0.1326	0.0521, 0.0745
resid. el. dens. [e Å ⁻³]	0.247/–0.247	2.140/–1.067	1.163/–1.306	1.637/–0.852	0.557/–0.708	0.341/–0.331

(NCH₃), 34.3 (NCH₃), 18.6 (C^{Me}-isonitrile) ppm. IR (KBr, cm⁻¹) 3055 (m), 3032 (m), 2960 (m), 2832 (m), 2155 (vs), 1963 (w), 1898 (w), 1823 (w), 1773 (w), 1603 (s), 1577 (m), 1504 (s), 1480 (s), 1443 (vs), 1387 (s), 1320 (w), 1231 (w), 1204 (w), 1131 (w), 1074 (vs), 1025 (s), 987 (s), 965 (m), 917 (s), 839 (vs), 773 (s), 698 (vs), 557 (s), 506 (w). Anal. Calcd for C₁₆₀H₁₃₆Cu₄N₂₂O₄P₂F₁₂·1.5CH₂Cl₂: C, 62.52; H, 4.52; N, 9.93. Found: C, 62.39; H, 4.59; N, 10.04. HR-MS (ESI, MeCN) calcd for [L³Cu₂(C₆H₃(CH₃)₂NC)₂]²⁺ 1340.41439, found 1340.41943; calcd for: [L³Cu]⁺ 1147.41915, found 1147.41933; calcd for: [H₂L³]⁺ 1085.49785, found 1085.49687.

Equilibrium Measurements. The purity of the ligand and the concentration of the ligand stock solution was determined by Gran's method.²⁸ The metal ion stock solutions were prepared from NiCl₂·6H₂O (Reanal) dissolved in doubly distilled water. ZnO (Reanal) was dissolved in a known amount of HCl solution (0.1 M). The concentration of the metal ion stock solutions was determined gravimetrically by precipitation of quinolin-8-olates. The HCl concentration of the Zn²⁺ solution and the exact concentration of the carbonate-free KOH titrant were determined by pH-potentiometry. pH-potentiometric titrations were performed in the pH range 2–11 or until precipitation occurred on samples of 4.00 cm³ at an ionic strength of 0.2 M (KCl) and at 25.0 ± 0.1 °C. During the titrations purified, strictly oxygen-free argon was continuously bubbled through the samples. The ligand concentrations were varied within the range 0.0015–0.002 mol·dm⁻³, and the metal to ligand ratios were 1:1 and 2:1 in all cases. The pH-metric titrations were performed with a Radiometer pHM84 instrument equipped with a Metrohm combined electrode (type 6.0234.100). Titrant KOH was added from a Metrohm 715 Dosimat auto burette. The electrode system was calibrated according to Irving et al.²⁹ so that the pH-meter readings could be directly converted

into hydrogen ion concentration. The water ionization constant (*pK_w*) obtained was 13.77 ± 0.01. The pH-metric results were utilized to find the stoichiometry of species and to calculate the stability constants. The calculations were made with the aid of the computer program PSEQUAD.³⁰ In the Ni²⁺ systems UV–vis measurements were performed at two analytical concentrations and two metal to ligand ratios. The ligand concentrations were 0.00135 and 0.00435 mol·dm⁻³, and the metal to ligand ratios were 1:1 and 2:1. A Perkin-Elmer Lambda 25 spectrophotometer was used to record the spectra in the region of 400–800 nm with a path length of 1 cm. The PSEQUAD program was used to calculate the individual spectra for the different Ni^{II}-containing complexes.³⁰

X-ray Crystallography. X-ray data were collected on a STOE IPDS II diffractometer (graphite monochromated Mo K α radiation, λ = 0.71073 Å) by use of ω scans at -140 °C (Table 4). The structures were solved by direct methods and refined on *F*² using all reflections with SHELX-97.³¹ Most non-hydrogen atoms were refined anisotropically, except some in disordered parts. Most hydrogen atoms were placed in calculated positions and assigned to an isotropic displacement parameter of 0.08 Å². The CO–H hydrogen atoms in **2a** and the O–H hydrogen atoms in **5** were refined without any restraints or constraints. Almost the same is true for the O–H hydrogen atom in **4**. Here the O–H distance was fixed using a DFIX restraint (*d*_{O–H} = 0.82 Å). The THP-group and one THF solvent molecule in **2a** were found to be disordered. The respective occupancy factors were refined to 0.677(5)/0.323(5)

(29) Irving, H.; Miles, M. G.; Pettit, L. D. *Anal. Chim. Acta* **1967**, *38*, 475–488.

(30) Zékány, L.; Nagypál, I. In *Computational Methods for the Determination of Stability Constants*; Leggett, D., Ed.; Plenum Press: New York, 1985; pp 291–353.

(31) (a) Sheldrick, G. M. *SHELXL-97, Program for Crystal Structure Refinement*; University of Göttingen: Göttingen, Germany, 1997. (b) Sheldrick, G. M. *SHELXS-97, Program for Crystal Structure Solution*; University of Göttingen: Göttingen, Germany, 1997.

(28) Gran, G. *Acta Chem. Scand.* **1950**, *4*, 559–577.

(THP), 0.55(2)/0.45(2) (THF). One water molecule appears to be partially occupied in the crystal structure of **2a**. It was refined with a fixed occupancy factor of 0.25. In **4** atoms of a nitrate anion and a diethyl ether molecule partially occupy the same sites. The nitrate could be refined on three positions with occupancies of 2×0.25 and 0.5. The occupancy of the diethyl ether molecule was set at 0.5. In case of the nitrate anion SADI (d_{N-O} and $d_{O...O}$) and FLAT restraints and EADP constraints and for the diethyl ether molecule DFIX ($d_{C-O} = 1.43 \text{ \AA}$ and $d_{C-C} = 1.51 \text{ \AA}$), DELU and SIMU restraints were used to control the geometry and displacement parameters. For the three disordered methanol molecules in **5** DFIX restraints ($d_{C-O} = 1.41 \text{ \AA}$) were applied to model the disorder. One methanol was refined on four positions (two of them are symmetry related) with occupancies factors of 0.25. The occupancy factors of the other two methanol molecules are 0.56(4)/0.44(4) and 0.518(15)/0.482(15). AFIX 66 was used to model the disorder of one phenyl ring in **6** (occupancy factors: 0.68(4)/0.32(4)) and two phenyl rings in **7** (occupancies factors: 0.514(7)/0.486(7) and 0.480(5)/0.520(5)). Additionally the PF_6^- anions in **7** are disordered (occupancy factors: 0.833(8)/0.167(8)). SADI (d_{P-F} , $d_{F...F}$) and EADP constraints were used to model the disorder. In **4** and **6–8**, the unit cell contains also disordered solvent molecules, for which no satisfactory model for the disorder was found: **4**:Et₂O; **6**:CH₂Cl₂/Et₂O; **7**:Et₂O; **8**:CH₂Cl₂. For further refinement, the contribution of the missing solvent molecules was subtracted from the reflection data by the SQUEEZE³² routine of the PLATON³³ program: **4**, 195.7 Å³, electron count 51; **6**, 967.2 Å³, electron count 185; **7**,

610.4 Å³, electron count 114; **8**, 558.6 Å³, electron count 96. Face-indexed absorption corrections for **5** ($T_{\text{max}}/T_{\text{min}} = 0.8889/0.7488$) were performed numerically with the program X-RED.³⁴

Acknowledgment. Financial support by the DFG (International Research Training Group GRK 1422 “Metal Sites in Biomolecules: Structures, Regulation and Mechanisms”), the Fonds der Chemischen Industrie, and the Hungarian Scientific Research Fund (OTKA T049612) is gratefully acknowledged.

Supporting Information Available: Crystallographic data, in CIF format, for **2a**, **4**, **5**, **6**, **7**, and **8**; ORTEP plots of **2a** (Figure S1), **4** (Figure S7), **5** (Figure S8), **6** (Figure S9), **7** (Figure S10), and **8** (Figure S11); color representation of the hydrogen bonding network of **2a** (Figure S2) and of the molecular structure of **8** (Figure S6); titration curve of HL¹ (Figure S3), and titration curves of HL¹ with Ni²⁺ (Figure S4) and Zn²⁺ (Figure S5, PDF). This material is available free of charge via the Internet at <http://pubs.acs.org>.

IC800248B

(32) Sluis, P. v. d.; Spek, A. L. *Acta Crystallogr.* **1990**, *A46*, 194–201.

(33) (a) Spek, A. L. *Acta Crystallogr.* **1990**, *A46*, C34. (b) Spek, A. L. *PLATON: A Multipurpose Crystallographic Tool*; Utrecht University: Utrecht, The Netherlands, 2006.

(34) *X-RED*; STOE & CIE GmbH: Darmstadt, Germany, 2002.